Russian Chemical Reviews **63** (7) 533 – 549 (1994)
©1994 Russian Academy of Sciences and Turpion Ltd

UDC 548.736

The structures of new germanates, gallates, borates, and silicates with laser, piezoelectric, ferroelectric, and ion-conducting properties

E L Belokoneva

Contents

I.	Introduction	533
II.	Brief characteristics of the methods for the preparation and study of the new compounds	534
III.	The garnet structural type	534
IV.	The $A_3M_xT_{6-x}O_{14}$ structural type	535
V.	The melilite structural type	537
VI.	The $Pb_3GeAl_{10}O_{20}$ and $NdAlGe_2O_7$ structural types	538
VII.	The stillvellite – datolite structural type in the $LnBGeO_5$ series	539
VIII.	Lanthanide borates with the huntite structure and their polytypic derivatives	540
IX.	The $KTiOPO_4$ structural type	541
X.	The sphene (titanite) structural type	545
XI.	Germanate-zeolites and zeolite-like germanates	546

Abstract. The results of studies on the structures of more than 50 new crystals of germanates, gallates, borogermanates, borates, and silicates, possessing laser, piezoelectric, ferroelectric, and ion-conducting properties, are presented. The structure–property relations are considered. The bibliography includes 71 references.

I. Introduction

The needs of modern engineering for new materials, which are promising by virtue of their unusual physical properties, are increasing with each year. Inorganic single crystals occupy an important place among such materials. The interest in them has been aroused by the developing modern technologies. Thus the enormous possibilities arising in the application of the new optical properties of crystals have been demonstrated in a communication [1] reviewing the results of studies involving the search for new nonlinear optical materials of the $KTiOPO_4$ structural type. The large band widths available in the optical transmission of data make it possible to move and store specimens with an information density in excess of 10^8 bits cm^{-2}. The generation of the third harmonic can be used to improve significantly the density of optical discs. The fibre optics used in telecommunications permits a relatively free transmission of signals subject to a minimal noise due to the external electromagnetic field. This also means that the modulations of the light wave carriers are nontrivial and that chemists specialising in materials science should play an important role in the creation of an optical system (crystal) with a predetermined amplitude and response time.

In a study [2] of the relation between the structures of new crystalline phases and their ferroelectric properties, the structure–properties problem was designated as crucial in chemistry and structural crystallography. Ferroelectrics, i.e. crystals capable of spontaneous polarisation, are materials in which structure–property relations are clearly manifested and are being actively investigated. Such materials frequently also possess ionic conductivity.

Studies in recent years have shown that solid electrolytes or superionic crystals have a specific structure — they contain large channel-cavities in which cations migrate. This has led to the specific search for and synthesis of such compounds.

Compounds in which, for example, luminescent, piezoelectric, and nonlinear optical properties are combined with a high mechanical and thermochemical stability are especially valuable. This review is devoted to the consideration of the characteristics of the steric structures of such compounds which have been obtained and whose structures have been investigated during the last 10 – 15 years. For example, in the case of solid state lasers, the search for compounds has been governed by problems involving the adoption of new spectral ranges and expansion of the stimulated radiation frequency ranges. Problems associated with the improvement of the effectiveness of energy conversion and of thermal stability are of current interest for piezoelectric single crystals.

The problem of the preparation of large and perfect single crystals for their subsequent study (in particular of their optical properties) and use is extremely important in such investigations. For this purpose, it is essential to know the conditions for the crystallisation of the corresponding phases. The determination of the regions of stability of structural types make it possible to achieve optimum compositions for the manifestation of the given physical properties by means of isomorphous substitution of atoms at different sites.

In the present review, attention is concentrated on the question of the relation between the structural characteristics of the new phases and physical properties. Mainly studies by Russian investigators, who have contributed greatly to the preparation and study of the properties and structures of new laser, piezoelectric, ferroelectric, and ion-conducting crystals, will be considered.

The majority of the germanate, gallate, and borogermanate crystals were obtained by B V Mill' in the Faculty of Physics at Moscow State University, the germanate-zeolites were obtained by L N Dem'yanets at the Institute of Crystallography of the Russian Academy of Sciences, and lanthanide borates were

E L Belokoneva Department of Crystallography and Crystal Chemistry, Faculty of Geology, M V Lomonosov Moscow State University, Vorob'evy gory, 119899 Moscow, Russian Federation.
Fax (7-095) 939 01 26. Tel. (7-095) 939 38 75

Received 28 April 1994
Uspekhi Khimii **63** (7) 559 – 575 (1994); translated by A K Grzybowski

prepared by L I Leonyuk in the Faculty of Geology at Moscow State University. The optical, piezoelectric, and mechanical properties were measured by A A Kaminskii and coworkers at the Institute of Crystallography of the Russian Academy of Sciences, while the measurements concerned with second harmonic generation and measurements of the electrical and ion-conducting properties were performed by S Yu Stefanovich of the Physicochemical Institute.

II. Brief characteristics of the methods for the preparation and study of the new compounds

The majority of the compounds, the crystals of which will be considered below, belong to the class of germanates and the related gallates. Crystallisation has been investigated for the $A_2O(AO)-M_2O_3(MO_2)-GeO_2(Ga_2O_3, SiO_2)$ systems, where A are alkali, alkaline earth, or lanthanide elements, i.e. large cations, and M are predominantly trivalent cations (Ga, Al, In, Fe, Sb, Ta), smaller in size and with higher electronegativities. The crystals were obtained by solid-phase synthesis,[3] i.e. by sintering in air-pressed mixtures of the oxides at 1100–1500 °C for 3–5 h (the temperatures used in the preparation of the single-phase specimens will be given below on the basis of the literature quoted in describing the data). The single crystals of a number of congruently melting compounds were grown by Czochralski's method. The boules were 8–9 cm long and 3 cm thick. The germanate-zeolites were obtained by hydrothermal synthesis[4] in autoclaves from alkaline solutions in the $NaAlO_2-GeO_2-Na_2CO_3-NaOH-H_2O$ systems at 300–500 °C. The lanthanide borates were synthesised by the solution-melt method in the $Ln_2O_3-Al_2O_3-B_2O_3-K_2Mo_3O_{10}$ systems by spontaneous crystallisation on cooling from 1500 °C.[5]

Crystalline elements in the form of rods up to 70 mm long and up to 5 mm in diameter with plane-parallel (5") end-faces were prepared for the investigation of the optical properties from the boules obtained by Czochralski's method.[6] The crystals were pumped by the pulsed radiation from neodymium (LaF_3, $Y_3Al_5O_{12}-Nd^{3+}$) and praseodymium ($Y_3Al_5O_{12}-Pr^{3+}$) laser crystals and also using Xe lamps. The spectral-lasing characteristics of the stimulated radiation, the optical transmission, absorption, and Raman spectra and the optical activity were investigated for the specimen synthesised, and measurements were also made of their elastic, dielectric, and piezoelectric characteristics. The measurements concerned with second harmonic generation and the measurements of the electrical and ion-conducting properties were performed by means of a specially developed method (see, for example, Belokoneva and Timchenko[5]).

Full X-ray diffraction studies of the single crystals of the new compounds were carried out in order to investigate their crystal structures. A correct allowance for the absorption of X-rays is extremely important in the study of objects containing germanium, gallium, the lanthanides, barium, strontium, and other heavy elements. In most cases, the single crystal specimens were prepared in the form of spheres with radii determined by the linear absorption coefficient ($\mu r \leqslant 4$).

The compounds will be considered in accordance with their structural types, most of which are known. New, previously unknown structural types or their modifications were also obtained and investigated in the course of the structural studies.

III. The garnet structural type

Many compounds with valuable properties crystallise with a garnet-type structure, for example, the garnet-ferrites $M_3Fe_5O_{12}$ with lanthanide elements at the dodecahedral M sites[8] or the familiar $Y_3Al_5O_{12}:Nd^{3+}$ laser crystal.[9] Isomorphous substitutions in the crystals can lead to the formation of new promising compounds.

By analogy with the work of Gibbs and Novak[10] on silicate garnets, in which the crystal-chemical characteristics and the region of stability were characterised as a function of the size of the ion at the dodecahedral (*c*) and octahedral (*a*) structural sites, the corresponding germanate analogues were investigated.[11] The garnet-germanate crystals were grown by Czochralski's method. The X-ray diffraction characteristics of the representatives of this series investigated are presented in Table 1. In the diffraction experiments, only the reflections for which the contribution of the cations is small or zero were scanned, this yielded from 58 to 86 observed independent reflections. The positional and thermal parameters of the O atom were refined on their basis, after which the interatomic distances in the polyhedra of the cations, located at the specific 24*c*, 16*a*, and 24*d* sites in the cubic lattice (the dodecahedron, octahedron, and tetrahedron) and their distortions were calculated. The quantities obtained from the structural data made it possible to deduce the region of stability of the germanium garnets (Fig. 1), i.e. to determine the combinations of ions in conformity with their ionic radii at the 24*c* and 16*a* sites of the *Ia*3*d* group when the germanium atoms are located at the 24*d* sites. These characteristics were deduced on the basis of the existence of common edges in the garnet structure between the tetrahedron and the octahedron, on the one hand, and the dodecahedra on the other.

Table 1. X-Ray diffraction characteristics of the phases investigated with the structure of the garnet type (space group *Ia*3*d*).

Compound	*a*/Å	μr	N_{refl}	R_{hkl} (%)
$Mn_3Al_2Ge_3O_{12}$	11.891(3)	2.5	84	7.8
$Ca_3Al_2Ge_3O_{12}$	12.116(3)	1.3	86	5.2
$Ca_3Ga_2Ge_3O_{12}$	12.247(3)	2.5	79	5.7
$Ca_3Fe_2Ge_3O_{12}$	12.338(3)	1.0	72	5.2
$Cd_3Sc_2Ge_3O_{12}$	12.449(3)	2.7	73	6.1
$Ca_3Sc_2Ge_3O_{12}$	12.506(3)	2.0	73	3.9
$Ca_3In_2Ge_3O_{12}$	12.595(3)	1.7	76	6.7
$Ca_3Lu_2Ge_3O_{12}$	12.738(3)	2.1	58	9.5
$Sr_3Sc_2Ge_3O_{12}$	12.750(4)	4.0	31	11.8

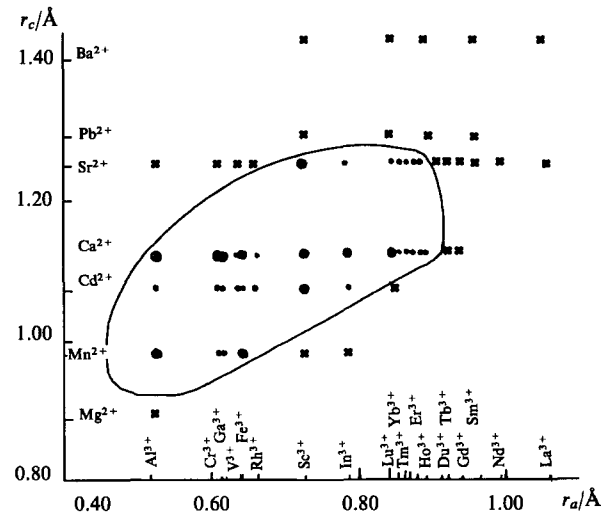


Figure 1. The region of stability of germanium garnets.

As regards practical applications (for the production of stimulated radiation), the $Ca_3Ga_2Ge_3O_{12}$ crystal activated by Nd^{3+} at concentrations from 0.05 to 16 at.% proved to be most promising. The position of the Nd^{3+}-activated ion was unambiguously determined as 24*c*, while that of the Cr^{3+} sensitiser ion was determined as 16*a*. The luminescence spectra of

this specimen have been analysed.[12] The question of the usefulness of polycationic garnets with heterovalent isomorphism for the formation of disordered Nd^{3+}-containing laser garnet crystals of the type $\{Ca_{1-x}Nd_x\}_3[Ga_2](Ge_{1-x}Ga_x)_3O_{12}$ was discussed in the same communication.

As a development of the possibilities of the heterovalent isomorphism discussed previously,[12] the cation-deficient garnet $Ca_{3.02}Nb_{1.67}Ga_{3.2}O_{12}$ (space group $Ia3d$, a = 12.507 Å) was synthesised and its structure was investigated.[13] The initial nonstoichiometry of the specimen compared with the standard $A_3B_2T_3O_{12}$ stoichiometry and also the unusually pronounced broadening of the lines in the luminescence spectra indicated a complex isomorphism and the presence of unoccupied cationic sites. Partial incorporation of Ca at the octahedral sites occupied predominantly by Nb and the excess Ga as well as the inclusion of a small proportion of Nb at Ga tetrahedral sites have been postulated. The ionic radii of the elements permit isomorphous mixing of this kind. In addition it was found that all the cationic sites in the structure are unoccupied. Successive refinement of various structural models of the crystal for different compositions (with specification of mixed atomic scattering curves) and populations of the atomic sites made it possible to obtain satisfactory thermal corrections for the atoms and the optimum divergence factor (R = 0.020) for the structural formula $\{\square_{0.05}.Ca_{2.95}\}[\square_{0.025}Ca_{0.07}Nb_{1.62}Ga_{0.275}](\square_{0.025}Nb_{0.05}Ga_{2.925})O_{12}$.

The existence of cationic vacancies was also established for V-garnets, but the Ca, Nb, Ga-garnet investigated by Kaminskii et al.[13] is the first disordered crystal with the garnet structure used to excite stimulated radiation. The statistical nature of the distribution of the heterovalent Ca^{2+}, Ga^{3+}, and Nb^{5+} ions among crystallographic sites, obtained as a result of X-ray diffraction study, was fully confirmed by the results of the study of the Raman spectra (Fig. 2), the luminescent properties, and the stimulated emission from this crystal containing Nd^{3+} ions. The high quality of experimental X-ray diffraction data and the reliability of the results for this crystal were confirmed by the investigation of the electron density distribution[14] and $\delta\rho$ maps, which proved to be comparable to those obtained for other garnets.

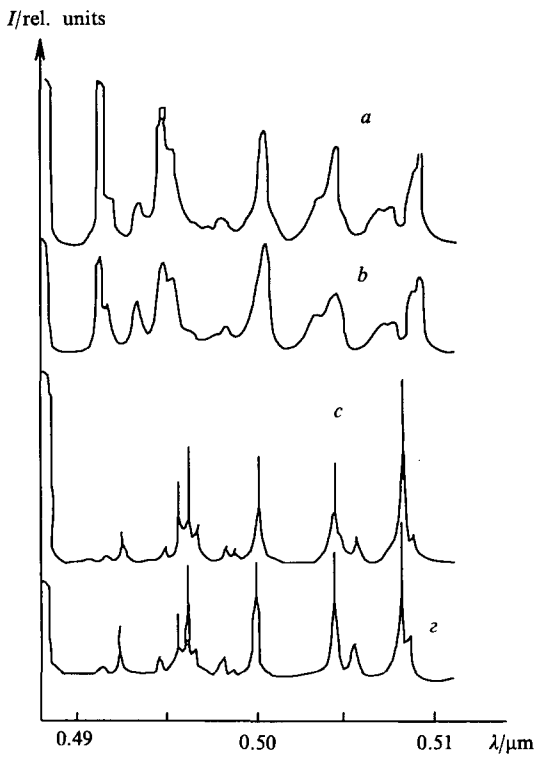


Figure 2. Raman spectra of the $Ca_{3.02}Nb_{1.67}Ga_{3.2}O_{12}$ garnets[13] with a disordered structure (a, b) and the $Ca_3Ga_2Ge_3O_{12}$ garnet with an ordered structure (c, d).

IV. The $A_3M_xT_{6-x}O_{14}$ structural type

In the study of the crystallisation of the $Ca_3Ga_2Ge_3O_{12}$ garnet, the compound $Ca_3Ga_2Ge_4O_{14}$ was obtained and subsequently became the parent compound of a series of compounds of a new structural type. The small amount of added oxides of certain tetravalent and pentavalent elements stabilises this new structural type for different compositions.[3] In the main, the compounds were obtained by solid-phase synthesis and those which melt congruently were synthesised by Czochralski's method. In all, more than 50 compounds were synthesised. The phase diagrams for the $CaO-Ga_2O_3-GeO_2$, $SrO-Ga_2O_3-GeO_2$, $Ln_2O_3-Ga_2O_3-SiO_2(GeO_2)$ (Ln = La, Nd), and $La_2O_3-Ga_2O_3-Nb_2O_5$ systems have been described.[15] The structures of seven compounds were investigated, the relevant data being presented in Table 2. In the acentric trigonal Fedorov group $P321$, which is characteristic of these phases, the cations are distributed among four regular point systems a, d, e, and f with different symmetries and with coordination to the oxygen atoms: a—octahedron with 32 symmetry; e—Thompson cube with 2 symmetry, and d and f—tetrahedra with 3 and 2 symmetry respectively (Table 2, Fig. 3). The true diffraction symmetry of $A_3M_xT_{6-x}O_{14}$ is trigonal ($P31m$), and the diffraction pseudosymmetry is hexagonal ($P6/mmm$). In the crystal structure, the Ge tetrahedra on the threefold and twofold axes form layers (Figs 3 and 4) perpendicular to the c axis. The Ge octahedra, strengthening the tetrahedra by forming a mixed framework, are distributed among them. The unshared ('hanging') apex of the d tetrahedron, viewed from above or downwards along the 3 axis (Fig. 3), makes it necessary to assign such a framework to the class of pseudoframeworks; the formula of the framework is $[M_1T_5O_{14}]$. The 'double-decker' structure of the framework is clearly seen in side projection (Fig. 4). The large A cations, the coordination polyhedra of which are the so called Thompson cubes in which the two square bases have been rotated relative to one another approximately by an angle of 45°, are located in the large cavities between the tetrahedral layers (Fig. 3). The most characteristic detail of the pseudoframework of the structural type considered is the group with 32 symmetry made up of the a octahedron and the three apices of the f tetrahedra linked to it.

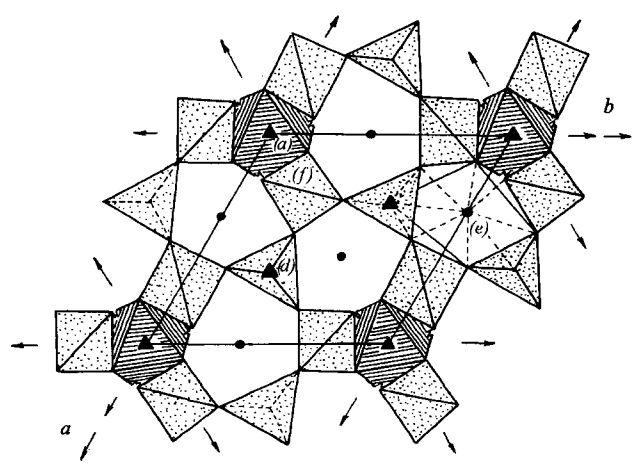


Figure 3. Projection of the crystal structure of the $A_3M_xT_{6-x}O_{14}$ type onto the ab plane. The regular systems of points for the positions of the cations and the symmetry elements are indicated.

Table 2. X-Ray diffraction characteristics of the phases investigated with structures of the $A_3M_xT_{6-x}O_{14}$ type.

Compound	a/Å	c/Å	Positions of cations[a]				μr	N_{refl}	R_{hkl} (%)
			e Thompson cube	a octahedron	d tetrahedron	f tetrahedron			
$Ca_3Ga_2Ge_4O_{14}$	8.076(3)	4.974(1)	Ca (2.549)	Ge (1.919)	Ge (1.752)	Ge+Ga=1:2 (1.826)	1.8	1516	6.3
$(Na_2Ca)Ge_6O_{14}$	8.183(3)	4.836(1)	Na+Ca=2:1 (2.579)	Ge (1.893)	Ge (1.747)	Ge (1.766)	2.2	1075	5.5
$Sr_3Ga_2Ge_4O_{14}$	8.270(3)	5.040(1)	Sr (2.654)	Ge+Ga=3:2 (1.924)	Ge (1.735)	Ge+Ga=7:8 (1.812)	3.7	1308	6.5
$Ba_3Fe_2Ge_4O_{14}$	8.541(5)	5.214(1)	Ba (2.783)	Fe (2.015)	Ge (1.763)	Fe+Ge=1:2 (1.812)	1.5	967	6.8
$La_3Ga_5SiO_{14}$	8.168(3)	5.095(1)	La (2.586)	Ga (1.997)	Ge+Si=1:1 (1.741)	Ga (1.861)	2.5	1979	4.5
$La_3Ga_5GeO_{14}$	8.204(4)	5.109(1)	La (2.592)	Ga (1.993)	Ga+Ge=1:1 (1.803)	Ga (1.852)	3.2	1693	4.0
$La_3Ga_{5.5}Nb_{0.5}O_{14}$	8.235(5)	5.129(2)	La (2.598)	Ga+Nb=1:1 (1.997)	Ga (1.829)	Ga (1.835)	2.4	1985	5.3

[a]The mean interatomic cation–oxygen distance (in Å) in the polyhedron is given in brackets.

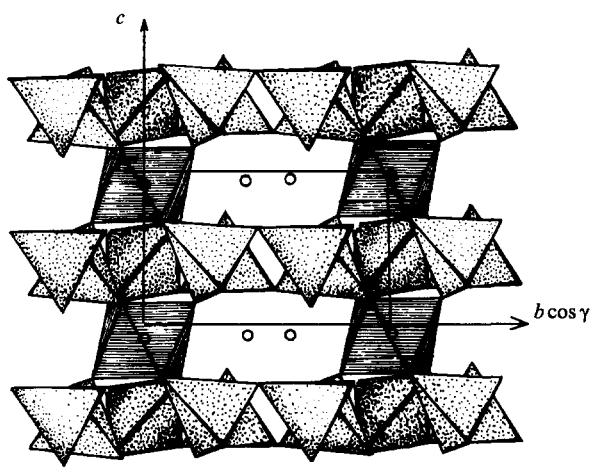


Figure 4. Projection of the crystal structure of the $A_3M_xT_{6-x}O_{14}$ type onto the *bc* plane.

Similar structural blocks are fundamental for mixed frameworks and pseudoframeworks of a large group of compounds with Ge atoms in octahedral and tetrahedral coordination such as $Li_2Ge_4O_9$, $LiNaGe_4O_9$, $Li_2Ge_7O_{16}$, $Li_4Ge_9O_{20}$, $Cd_2Ge_7O_{16}$, $BaGe_4O_9$, $K_2Ba(Ge_4O_9)_2$, and $Ba_3Ge_9O_{20}(OH)_2$.[16] The symmetry of the microblocks may be varied: 32, $\bar{3}m$, $3m$, $\bar{3}$, i.e. they may or may not have a centre of symmetry.

A similar structure, involving the existence of layered tetrahedral elements and different combinations of tetrahedra and octahedra, is characteristic of a large group of germanates, which nevertheless differ in the symmetry of their structures (the tetragonal Cd germanate, the trigonal Ca, Ga and K, Ge germanates, the orthorhombic $Li_2Ge_4O_9$ and $Li_2Ge_7O_{15}$, and the monoclinic $Li_4Ge_9O_{20}$) and in the topology of the tetrahedral layer. The axes perpendicular to the layered elements have the same dimensions in all the structures as that of the c = 4.7 Å axis of the structural type investigated or are a multiple of it (Fig. 5).

All these phases contain large interlayer cavities which can be filled by cations. Such cavities constitute convenient sites for activator ions. This can lead to the appearance of laser properties in the crystal. One can also postulate that phases such as $Cd_2Ge_7O_{16}$ (sp. gp $P\bar{4}b2$), $BaGe_4O_9$ (sp. gp $P31m$),

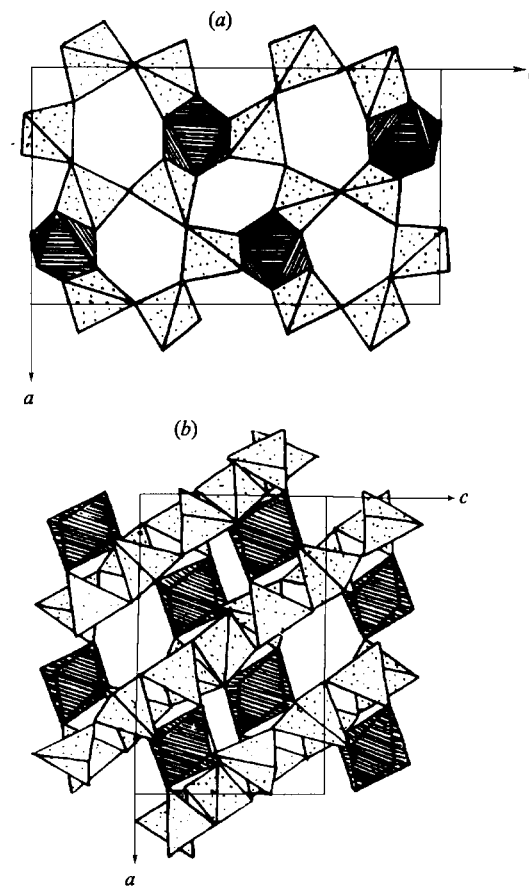


Figure 5. The crystal structures of $Li_2Ge_4O_9$ (*a*) and $Li_4Ge_9O_{20}$ (*b*). The anionic framework is illustrated.

and $Li_4Ge_9O_{20}$ (sp. gp $C2_1$) are promising as regards possible ferroelectric (for polar crystals) properties. Thus it has been established[17] that the compound $Li_2Ge_7O_{15}$ in this group undergoes a phase transition at 283.5 K ($Pbcn$—$Pbc2_1$) to a polar ferroelectric modification, which is accompanied by spontaneous polarisation along the c axis of the structure.

The synthesis and X-ray diffraction structural studies established that in crystals of the $A_3M_xT_{6-x}O_{14}$ structural type there is a possibility of extensive isovalent and heterovalent isomorphism which would enhance the laser and piezoelectric properties of those crystals which possess them.

The region corresponding to the stability of the compounds has been constructed in accordance with the crystal-chemical results in terms of the radii of ions with C.N. = 8 and the average radii of the ions of the framework as variables (Fig. 6).[16] Table 2 shows that isomorphic substitutions take place at all the cationic structural sites: (Na + Ca), Ca, Sr, Ba, and La for *e*; Ge, (Ge + Ga), Fe, and (Ga + Nb) for *a*; Ge, (Ga + Si), and Ga for *d*; Ge, (Ge + Ga), (Fe + Ge), and Ga for *f*. In the presence of isomorphism, the charge on the framework varies from −4 to −9: $[Ge_6O_{14}]^{4-}$, $[Ga_2Ge_4O_{14}]^{6-}$ and $[Fe_2Ge_4O_{14}]^{6-}$, $[Ga_5SiO_{14}]^{9-}$. One of the two independent tetrahedra, the *f* tetrahedron on the twofold axis, forming a microblock with the octahedron, is larger than the *d* tetrahedron on the threefold axis. In the *f* tetrahedron, the average interatomic distance varies from 1.766 Å (Ge) to 1.861 Å (Ga) with a possible inclusion at this site of up to 30% of the Fe atoms ($Ba_3Fe_2Ge_4O_{14}$). (In the structurally similar tetragonal gehlenites, which will be considered below, there is also a difference between the sizes of the two independent tetrahedra.) The tetrahedron on the threefold axis represents a cell for the smallest cations in the given structural type, in particular for Si^{4+} in $La_3Ga_5SiO_{14}$.

Octahedra with a mixed framework are also distinguished by 'flexibility' as regards size [the mean cation–oxygen distance varies from 1.893 Å (Ga) to 2.015 Å (Fe)] and, as already noted, can be occupied by germanium, gallium, niobium (to the extent of 50%), and iron cations. The fairly loose framework which is susceptible to isomorphism is readily distorted, and this may be the reason for the appearance of polarity in the structure and of the spontaneous polarisation vector P_s. The introduction of the Nd^{3+} activator ion at sites with lanthanide elements makes it possible to obtain satisfactory lasing characteristics.[18] The compound $La_3Ga_5SiO_{14}$ proved to have the best spectroscopic characteristics and piezoelectric properties among all those investigated.[3,15] $La_3Ga_5SiO_{14}$ single crytals are nowadays grown by a number of western and Russian firms. In accordance with the structural results, these crystals have been assigned to the class of materials with a disordered structure and a single activation quasi-centre. The fully substituted (La^{3+}–Nd^{3+}) compound $Nd_3Ga_5SiO_{14}$, i.e. a compound with a very high Nd^{3+} concentration, has been obtained from $La_3Ga_5SiO_{14}$.[6] Crystals of lanthanum gallate containing niobium (Table 2), which is incorporated in the *a* octahedron, are promising as regards the manifestation of nonlinear optical properties.

All the crystals of this group exhibit a piezoactivity higher by a factor of 3–8 than that of quartz.[15] The acoustic Q-factor of the crystals is also higher. Although the symmetry space groups of the new phases ($P321$) and quartz ($P3_121$) differ, they are both acentric and belong to the same 32 point group.

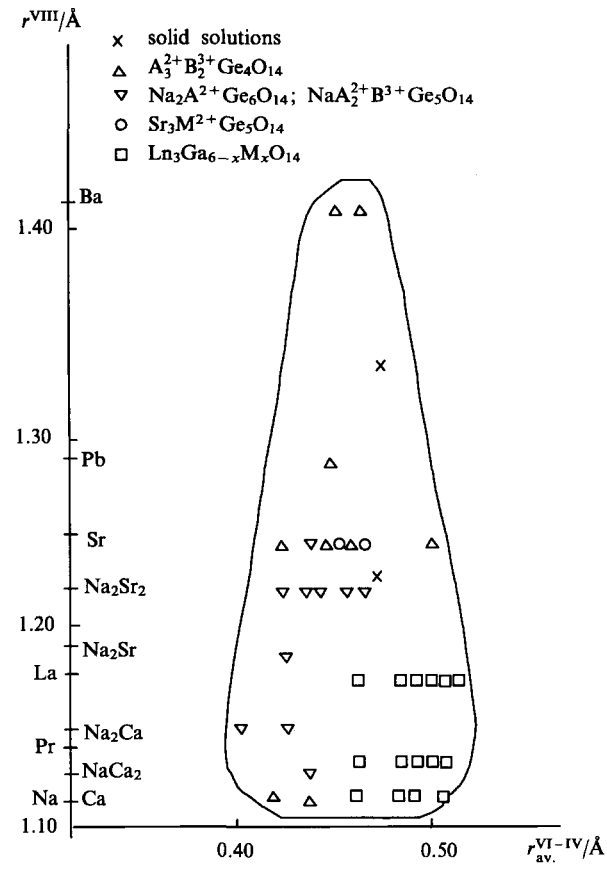


Figure 6. The region of stability of the compound $A_3M_xT_{6-x}O_{14}$.

The unique combination of physical properties (luminescent, laser, nonlinear optical, piezoelectric, and elastic) in this structural type of germanates makes it possible to regard them as multifunctional elements for technological purposes.

V. The melilite structural type

In the study of the $CaO-Ga_2O_3-GeO_2$ ternary system, crystals of the Ca, Ga, Ge-gehlenite $Ca_2Ga_2GeO_7$, belonging to the melilite structural type, were obtained. The interest in compounds with the melilite structure is due to the fact that stimulated emission from Ba,Zn and Ba,Mn germanates with the melilite structure and containing Nd^{3+} ions has been excited. A structural study of $Ca_2Ga_2GeO_7$ confirmed[19] that it belongs to the melilite structural type with the $P\bar{4}2_1m$ group. Apart from this compound, two further representatives of this structural type have been

Table 3. X-Ray diffraction characteristics of the phases investigated with structures of the gehlenite type.

Compound	*a*/Å	*c*/Å	Positions of cations[a]			μr	N_{refl}	R_{hkl} (%)
			e Thompson cube	*a* tetrahedron	*e* tetrahedron			
$Ca_2Ga_2GeO_7$	7.896(4)	5.207(2)	Ca (2.58)	Ga (1.85)	Ga + Ge = 1 : 1 (1.80)	0.9	392	5.5
$Ca_2Ga_2SiO_7$	7.793(3)	5.132(2)	Ca (2.580)	Ga (1.815)	Ga + Si = 1 : 1 (1.723)	0.8	722	4.2
$CaNdGa_3O_7$	7.903(3)	5.231(2)	Ca + Nd = 1 : 1 (2.591)	Ga (1.816)	Ga (1.824)	2.35	842	5.2

[a]The mean interatomic cation–oxygen distance in the polyhedron (in Å) is given in brackets.

synthesised and their structures have been investigated—$Ca_2Ga_2SiO_7$ and $CaNdGa_3O_7$ (Table 3)[20] (the low accuracy of the structural data obtained previously[21] for $Ca_2Ga_2SiO_7$ precluded a complete interpretation of the physical properties). The calcium or calcium + neodymium cations in the compounds synthesised are accommodated in Thompson cubes with the *m* symmetry. The larger *a* tetrahedra on the inversion axes, filled in the given structures with gallium atoms, are occupied by magnesium atoms in melilites and by iron atoms in åkermanites. The smallest *e* tetrahedra with *m* symmetry are occupied by Ga, Ga + Ge, and Ga + Si. The cationic polyhedra of gehlenites and $A_3M_xT_{6-x}O_{14}$ are identical (Tables 2 and 3). Despite the significant difference between symmetries (trigonal and tetragonal), the two structural types of Ca gallogermanates have features in common as regards coordination polyhedra, isomorphous relations (Tables 2 and 3), and the alternation along the *c* axes of layers of tetrahedra and A polyhedra in the large interlayer cavities.

The increased germanium content in the trigonal phase revealed, as mentioned previously by many investigators, its amphoteric nature, cationic character, and the manifestation of the octahedral as well as tetrahedral environments. The tetrahedral layers of both gallogermanates also have similar structures. The tetrahedral melilite layer can be described as made up of translationally identical bands extended along the *a*(*b*) axis (Fig. 7*a*). Five-membered tetrahedral rings can be distinguished in each band. The tetrahedral layer in the trigonal phase is made up of similar bands twisted in succession around the 2 axes (Fig. 7*b*). As a result of the presence of germanium atoms in the octahedra in this structure, the tetrahedral five-membered rings are ruptured and the band is converted into a chain. One of the melilite tetrahedra has rotated and occupies a position on the 2 axis (Fig. 7*b*). The relative dimensions of both *a*(*b*) axes and the *c* axis in both structures are in full agreement.

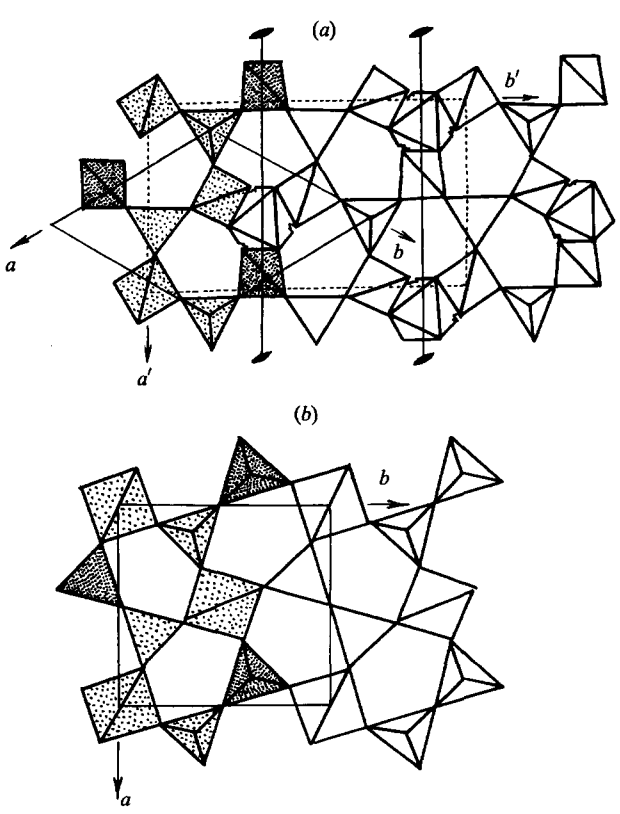


Figure 7. Comparison of the structures of $Ca_3Ga_2Ge_4O_{14}$ (*a*) and $Ca_2Ga_2GeO_7$ (*b*).

Thus the similar crystal structures involving the presence of layered elements and large cavities between them—the positions of the cations A and the impurity activator ions Nd^{3+}—made it possible to use the crystals of both structural types in lasers. Stimulated emission has been investigated.[20] According to X-ray diffraction data, crystalline $Ca_3Ga_2Ge_4O_{14}$ and $Ca_2Ga_2GeO_7$ are disordered compounds with a single activation quasi-centre.

VI. The $Pb_3GeAl_{10}O_{20}$ and $NdAlGe_2O_7$ structural types

The compound $LaSr_2Ga_{11}O_{20}$ crystallises in the $SrO-La_2O_3-Ga_2O_3$ system and its structure is similar to that of $Pb_3GeAl_{10}O_{20}$ (Table 4).[22] The results of an X-ray diffraction study showed that the Ga atoms, like the Ge and Al atoms in the structure of the prototype phase, form a mixed framework. It is made up of Ga octahedra joined into bands and Ga tetrahedra forming a highly puckered three-dimensional double-decker layer with large cavities (Fig. 8). In the tetrahedral layer, it is possible to distinguish vinogradovite bands linked in pairs by the mirror *m* planes (Fig. 8). In the cavities of the mixed framework, which has many features in common with the vinogradovite structure, there are two sites for the large La and Sr cations: sites *a* (2/*m* symmetry) at which Sr atoms are located and *i* sites (*m* symmetry) occupied isomorphously by the La and Sr atoms in proportions of 1 : 1. Calculation of the mean interatomic distances showed that a Sr–O distance of 2.691 Å is characteristic of the larger *a* cavity (distorted octahedron), whereas in the heptagon of the *i* site the mean (La, Sr)–O distance is 2.628 Å. It follows from X-ray diffraction data that the Nd^{3+} activator ion occupies the 4*i* site. The La–Sr disorder is manifested also in spectroscopic data.[22] Analysis of the parameters of the anisotropic thermal vibrations shows that the Sr atoms vibrate more freely in the *bc* plane in the intertetrahedral layer, whereas the Sr, La atoms vibrate in the direction of the *c* axis in the communicating open-network cavities (Fig. 8). The La,Sr gallate, which appears promising for use in lasers, has structural features in common with $A_3M_xT_{6-x}O_{14}$—a mixed framework made up of octahedra and tetrahedra with large cavities for identical large cations.

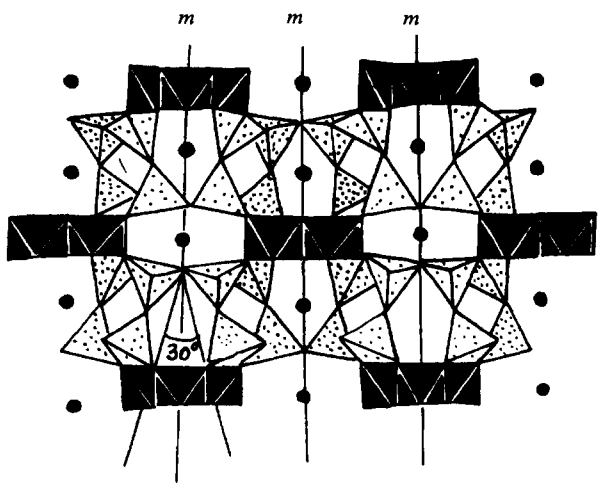


Figure 8. The crystal structure of La,Sr gallate.

Crystals of $LaGaGe_2O_7$ have been obtained in the study of the conditions for the crystallisation of $La_3Ga_5GeO_{14}$ in the $La_2O_3-Ga_2O_3-GeO_2$ system. X-Ray phase analysis[23] showed that they belong to the $NdAlGe_2O_7$ structural type. X-Ray structural study of the single crystals (Table 4) confirmed this similarity. Apart from the La gallogermanate, the Gd gallogermanate was obtained and its structure was investigated (Table 4). In the

Table 4. X-Ray diffraction characteristics of the phases investigated with structures of the $Pb_3GaAl_{10}O_{20}$ and $NdAlGe_2O_7$ types.

Compound	a/Å	b/Å	c/Å	β	Space group	μr	N_{refl}	R_{hkl} (%)
$LaSr_2Ga_{11}O_{20}$	14.576(5)	11.637(3)	5.070(1)	91.27	$I2/m$	2.4	2319	4.3
$LaGaGe_2O_7$	7.307(2)	6.635(1)	12.962(4)	117.41	$P2_1/c$	2.9	3419	7.3
$GdGaGe_2O_7$	7.160(3)	6.571(2)	12.763(4)	117.5	$P2_1/c$	2.0	3212	3.8

crystal structures of both phases, the Ge tetrahedra, combined into diortho-groups, and the Ga pentagons (distorted trigonal bipyramids) form a mixed framework as in the phases investigated previously. It is possible to distinguish in them six-sided window-rings made up of two Ga pyramids and two diortho-groups $[Ge_2O_7]$ as well as four-sided window-rings made up of two tetrahedra and two Ga pyramids (Fig. 9). The lanthanide cations (La, Gd), C.N. = 9, coordinated to O atoms are accommodated in the large cavities. The interatomic distances are La–O = 2.558 Å and Gd–O = 2.481 Å. When the crystals were activated by Nd^{3+} ions, occupying the sites for the lanthanide element, stimulated emission was obtained.[23,24]

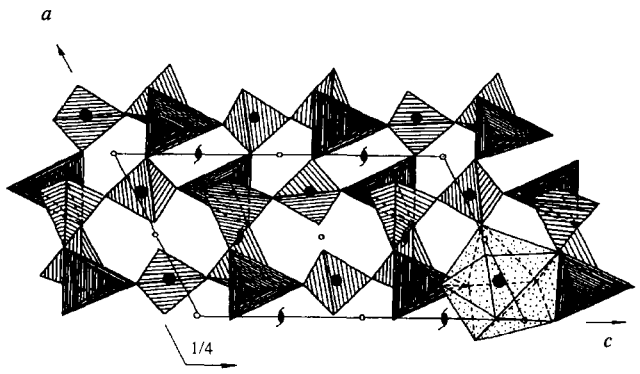


Figure 9. Projection of the crystal structure of $LaGaGe_2O_7$ onto the *ac* plane.

VII. The stillvellite–datolite structural type in the $LnBGeO_5$ series

In terms of their structures, the compounds $LnBGeO_5$ are divided into two groups: compounds with Ln = La–Pr (at low temperatures also with Nd and Eu), which crystallise with the structure of the type of the mineral stillvellite $CeBSiO_5$; the compounds with Ln = Nd–Er and Y (with Nd–Eu in the high-temperature form) have a monoclinic structure, which was assumed similar to that of stillvellite before a structural study had been carried out.

The crystal structures of $LaBGeO_5$ and $NdBGeO_5$ have been investigated.[25] The stillvellite structural type with the $P3_1$ polar space group has been confirmed for $LaBGeO_5$ (Table 5). In a study of the structure of stillvellite, it had been noted earlier[26] that it has a pseudosymmetry corresponding to the space group $P3_121$ but photographic experimental data and extremely limited diffractometer data cast doubts on the correctness of the choice of the space group $P3_1$ and precluded the determination of the deviations from the pseudosymmetry. The determination of the crystal structure of $LaBGeO_5$ made it possible to achieve this.

The positions of the heavy La and Ge atoms are very similar to the specific positions on the twofold axes in the space group $P3_121$,[24] in which the O(1, 2) and O(3, 4) atoms are linked in pairs by the twofold axes. The B and O(5) atoms are furthest away from the postulated specific positions on the twofold axes of the space group $P3_121$ and remain independent (Fig. 10). According to the literature,[27–29] the phase transition observed at T_c = 530 °C may correspond to the phase transition from the space group $P3_1$ to the space group $P3_121$ with loss of polarity by the crystals but with retention of acentricity. We may note that deviations from pseudosymmetry are significant for all the atoms in the $LaBGeO_5$ structure at room temperature and appreciably exceed the errors.[25]

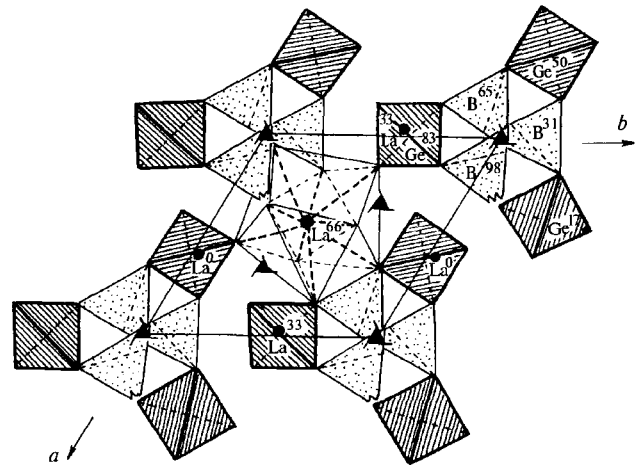


Figure 10. Projection of the crystal structure of $LaBGeO_5$-stillvellite onto the *ac* plane.

The $P3_1$–$P3_121$ phase transition belongs to the class of second-order phase transitions of the displacement type. The $LaBGeO_5$ structure can be described as made up of columns of La nonagons and Ge tetrahedra (Fig. 10) extended along the c axis. Chains made up of $[BO_4]$ tetrahedra, forming together with the Ge tetrahedra the $[BGeO_5]$ chain radical, are extended between the columns in the same direction along the c axis.[26] In an independent accurate study of the crystal structure of stillvellite,[30] difficulties were noted in refining the positional and thermal parameters of the O(5) atom and additional electron density peaks in the vicinity of this atom were observed. The authors[30]

Table 5. X-Ray diffraction characteristics of the $LaBGeO_5$ phases investigated with structures of the stillvellite and datolite types.

Compound	a/Å	b/Å	c/Å	β	Space group	μr	N_{refl}	R_{hkl} (%)
$LaBGeO_5$	7.020(5)	–	6.879(4)	–	$P3_1$	0.95	1407	2.9
$NdBGeO_5$	10.048(20)	7.610(10)	4.964(7)	92.0	$P2_1/a$	3.00	2367	3.0

concluded that the crystal investigated is twinned and is obtained as a result of rotation about an axis along the [110] direction. The polar individuals are linked in opposite directions along the c axis, their volumes amounting to 0.605 and 0.395 respectively.

Numerous studies of the physical properties of the $LaBGeO_5$ crystal, in particular the laser, nonlinear optical,[31] and ferroelectric[28,29] properties, have shown that this material possesses all three properties. For example, the intensity of the generation of the second harmonic in this crystal exceeds by a factor of 50 the intensity in $La_3Ga_{5.5}Nb_{0.5}O_{14}$ (see above). The possibility of obtaining large high-quality single crystals from the melt constitutes an advantage of $LaBGeO_5$ over, for example, other likely materials for the creation of effective lasers with self-multiplication of the lasing frequency, such as $LiNbO_3$ and $YAl_3(BO_3)_4$ with Nd^{3+}. Structural data make it possible to explain the occurrence of the spontaneous polarisation P_s in the given crystal and its ferroelectric properties.

The crystal structure of $NdBGeO_5$ differs from that of stillvellite[25] but is close to the structure of another natural borosilicate—datolite $CaBSiO_4(OH)$ and it involves the replacement in the latter of Ca by Nd, of Si by Ge, and of OH^- by O^{2-}. It can be described as a layered structure (Fig. 11) in which the large-cation layers alternate with tetrahedral layers along the c axis. Tetrahedral layers, the structure of which is similar to that of the datolite layers, are also present in melilite, the structural type of which was described above. A similarity between the melilite and $A_3M_xT_{6-x}O_{14}$ layers was noted at the same time (Fig. 7). The Nd and Ca coordination polyhedra are identical—they are all the same Thompson cubes. As regards the manifestation of physical properties, the presence of the centrosymmetrical space group for members of the lanthanide series ranging from Nd and beyond rules out the nonlinear optical and ferroelectric properties, but the possibility of the manifestation of laser properties is retained.

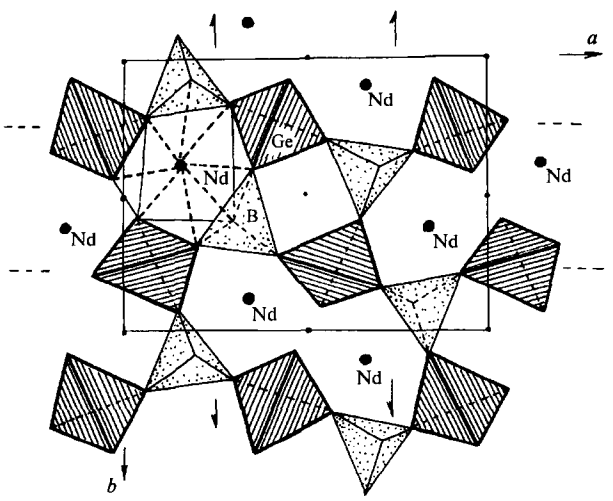


Figure 11. Projection of the crystal structure of $NdBGeO_5$-datolite onto the *ab* plane.

Two polymorphic modifications of $LnBGeO_5$—the chain (stillvellite) and layered (datolite) modifications—have significantly different structures. The polymorphism of $LaBGeO_5$ is associated with the variation of the sizes of the Ln^{3+} ions (the lanthanide contraction). The stillvellite structure is characteristic of compounds with large ions accommodated in coordination polyhedra (nonagons), whereas for members of the series with smaller ions, the stability of the stillvellite structure diminishes and in the datolite structure the coordination polyhedra are octagons—Thompson cubes. Both structures obtain for cations of average size ($Nd^{3+}-Eu^{3+}$).

The sharp difference between the structures of the two polymorphic modifications of $LnBGeO_5$ is manifested in absorption luminescence spectra.[25] In both structures, the Nd^{3+} ions form activator centres of the same type. On the other hand, the coordination numbers, coordination polyhedra, and the symmetries of sites differ markedly in the structures of these centres. In conformity with the structural results, the spectroscopic data show that both phases belong to the class of simple crystals with an ordered structure.

VIII. Lanthanide borates with the huntite structure and their polytypic derivatives

The compound $YAl_3(BO_3)_4:Nd^{3+}$ with the huntite $CaMg_3(BO_3)_4$ structure already attracted the attention of investigators a long time ago—since the beginning of the 1960s. The crystals of Y,Al-huntite possess a combination of laser and nonlinear optical properties.

Studies on the solution-melt crystallisation of the Y, Al borate made it possible to obtain crystals of this compound of satisfactory quality; structural studies have been carried out for the compounds $NdAl_3(BO_3)_4$[32] and $GdAl_3(BO_3)_4$,[33] directly for $YAl_3(BO_3)_4$,[34] and also for $NdGa_3(BO_3)_4$[35] and $(Nd,Bi)Fe_3(BO_3)_4$.[36] It was observed that, apart from the huntite modification,[34–36] further monoclinic high-temperature modifications[32,33] are characteristic of $LnAl_3(BO_3)_4$. They were investigated in relation to $NdAl_3(BO_3)_4$ and $GdAl_3(BO_3)_4$. The crystallisation regions of the high-temperature modifications of the neodymium and gadolinium borates differ appreciably. The high-temperature monoclinic modification of the Nd,Al borate is stable over a wide temperature range (from 870 to 1150 °C). The high-temperature monoclinic modification of Gd,Al borate was noted in the crystallisation of highly supersaturated solution-melts at a temperature above 1060 °C. It was shown[5] that the two monoclinic modifications of Nd,Al and Gd,Al borates are different polytypic modifications having the same parameters a and b but different parameters c, structures, and space groups (Table 6).

In the rhombohedral cell of huntite, it is possible to select the monoclinic C cell in accordance with familiar rules. One of the $a(b)$ axes of the trigonal cell then becomes the monoclinic axis, one of the R translations becomes a C translation, and the a and c axes with the corresponding angle β may be selected on the basis of the R lattice sites in the plane perpendicular to b. In both monoclinic borates, it is possible to select cells with the same monoclinic angle β in which the parameters c'_2 and c'_3 are greater by factors of 2 and 3 respectively than the parameters c'_1 of the huntite modification ($c'_1 = 5.9$ Å) considered in the monoclinic aspect.

Dornberger-Schiff[37] devised a theory of OD structures the symmetry relations of which have been applied widely and clearly for the description of the characteristics of polytypic structures with differentiation of one or more types of layers and consideration of different kinds of neighbours. Thus it is possible to differentiate layers of two types (L_{2n} and L_{2n+1}; Fig. 12) in the monoclinic cells of three modifications of lanthanide borates (huntite, Nd,Al and Gd,Al borates). The layers of the first type (L_{2n}) are made up of pairs of edge-linked Al octahedra combined by B triangles into a layer. The formula of the layer is $[Al_2B_2O_{10}]$ and its symmetry is higher than that of each structure and can be described in terms of the $C2/m$ symmetry group. Layers of the second type (L_{2n+1}) are made up of Ln trigonal prisms and Al octahedra linked via their apices into columns extended along the a axis; the columns are also bound by the B triangles. The formula of the layer is $[LnAlB_2O_{10}]$ and its symmetry is $C2$. When two layers are combined in the structure, sixteen oxygen atoms are shared and a compound with the formula $LnAl_3B_4O_{12}$ is obtained. The subsequent odd L_{2n+1} layers are obtained from the initial layer by multiplication involving symmetry operations on the even L_{2n} layers: by the twofold axes in the case of huntite, by the centres of symmetry $\bar{1}$ in the case of Nd,Al borate, and by the twofold axes and the centres of symmetry $\bar{1}$ simultaneously with the

Table 6. X-Ray diffraction characteristics of the $LnAl_3(BO_3)_4$ phases investigated.

Compound	a/Å	b/Å	c/Å	β	Space group	μr	N_{refl}	R_{hkl} (%)
$YAl_3(BO_3)_4$	9.295(3)	–	7.243(2)		$R32$	0.8	450	3.7
$NdGa_3(BO_3)_4$	9.500(1)	–	7.502(2)		$R32$	2.0	464	3.0
$(Nd_{0.5}Bi_{0.5})Fe_3(BO_3)_4$	9.587(3)	–	7.608(2)		$R32$	2.4	654	3.9
$NdAl_3(BO_3)_4$	7.262(3)	9.365(3)	11.138(7)	103.41	$C2/c$	1.4	3641	5.0
$GdAl_3(BO_3)_4$	7.262(3)	9.315(3)	16.184(4)	90.37	$C2$	1.5	5063	5.2

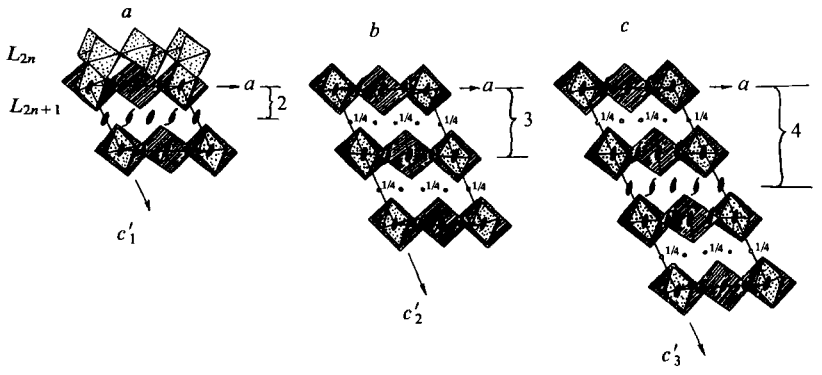


Figure 12. Polytypic diversity in the family of Ln,Al borates: (*a*) huntite (222...); (*b*) the Nd,Al modification ($\bar{1}\bar{1}\bar{1}$...); (*c*) the Gd,Al modification ($\bar{1}\bar{1}2\bar{1}\bar{1}2$...).

$\bar{1},\bar{1},2,\bar{1},\bar{1}$... alternation in the case of Gd,Al borate. Thus the odd layers in the structures with the C_2 symmetry are multiplied by the $C2$ and $C\bar{1}$, subgroups belonging to the $C2/m$ group of the even layer.

L_{2n}	L_{2n+1}
$[Al_2B_2O_{10}]$	$[LnAlB_2O_{10}]$
$C\ 1\ 2/m$ (1)	$C\ 1\ 2$ (1)
$[P\ 1\ 2$ (1)]	$[C\ 1\ 2/\bar{1}$ (1)]

The result obtained expresses the operation of the familiar Dornberger-Schiff theorem, according to which the number of combinations of two layers Z is equal to the ratio of the multiplicity of the symmetry group of the initial layer N and the multiplicity F of the symmetry group of a pair of layers, i.e. $Z = N/F$. In the given case, $Z_{2(1)} = 4/2 = 2$. The sequence 222... corresponds to a structure with a period c in one pair of layers (Fig. 12, braces) — this is the huntite structure, which can be described in terms of the rhombohedral setting. The sequence $\bar{1}\bar{1}\bar{1}$... corresponds to a structure with a period c in two pairs of layers — this is the high-temperature $NdAl_3(BO_3)_4$ modification. The sequence $T\ \bar{1}\bar{1}2\bar{1}\bar{1}2$... corresponds to the third, $GdAl_3(BO_3)_4$ structure and has a period in three pairs of layers.

The different sequences of operations afford hypothetical structures with different periods and symmetries. The possible variants for 10-layer polytypes with a symbolic-literal description have been specified by Zvyagin and Belokoneva. [38]

The Laue diffraction patterns for Nd huntite, obtained (in contrast to the remaining lanthanide borates) by rapid quenching, showed, together with point reflections also distinct diffuse reflections. Out of the three equally legitimate a axes in the trigonal cell, one axis, which possesses a plane of symmetry according to the diffuse reflections, was selected. The $h0l$ and $h1l$ layer lines, corresponding to the monoclinic setting of the trigonal phase, were recorded along this axis. Distinct diffuse lines, along which the index l varies continuously, were observed on the Weissenberg diffraction pattern. Point reflections, corresponding to integral values of l for c in the huntite structure were distinguished against their background. This type of picture indicates the breakdown of a rigorous order in the alternation of layers and the existence of a disorder superimposed on the ordered structure.

It is seen from the foregoing that the decisive factors in the formation of borate polytypes and in the breakdowns of order in the latter are the crystallisation temperatures and the rate of cooling of the melt. The higher the crystallisation temperature, the more complex the polytypes. Polytypes even more complex than those established hitherto may be found among them. Strictly ordered polytypes are formed on slow cooling, while at a high cooling rate a nonordered structure also arises against the background of the simplest ordered structure (as in trigonal huntite)

The nature of the lanthanide element also plays a definite role in polytypicism. It has been noted [39] that the statistics of the morphotropic transitions in tetrahedral compounds (silicates, germanates, phosphates) with lanthanide elements makes it possible to differentiate a single common region around Nd (in the case of germanates this also applies to Gd). The $LnBGeO_5$ and $LnAl(BO_3)_4$ series provide a good illustration of the empirical rule noted above. The reason for it is the magnitudes of the ionic radii of the lanthanide elements.

The phase transitions between the polytypic modifications examined above, which occur at different temperatures and sometimes coexist (for example, in the case of Pr, Al borate [40]) are second-order phase transitions of the 'order–disorder' type and are accompanied by very slight changes in structure.

Structural studies made it possible to account for the absence of nonlinear optical properties in $NdAl_3(BO_3)_4$, unlike $YAl_3(BO_3)_4$, and also for the impairment of their laser properties†. The former is associated with the presence in the Nd,Al borate crystals of the monoclinic centrosymmetric space group $C2/c$, while the latter is associated with the polytypic nature of the phases, which entails a tendency towards disorder and inhomogeneity in the crystal, particularly with increase in the crystallisation temperature.

IX. The $KTiOPO_4$ structural type

Potassium titanyl phosphate $KTiOPO_4$ (PTP) is nowadays one of the most effective nonlinear optical crystals. [1] The germanate and silicate analogues of $KTiOPO_4$ having the general formula

† In all the crystals, the positions of the activator ions correspond to the positions of Ln or Y.

Table 7. X-Ray diffraction characteristics of the phases investigated with structures of the $KTiOPO_4$ type.

Compound	a/Å	b/Å	c/Å	Space group	μr	N_{refl}	R_{hkl} (%)
$KSbOGeO_4$	13.224(2)	6.597(1)	10.759(2)	$Pna2_1$	1.35	3044	2.6
$KTaOGeO_4$	13.386(3)	6.658(3)	10.997(2)	$Pna2_1$	3.10	2110	3.3
$RbNbOGeO_4$	13.382(3)	6.708(2)	10.746(2)	$Pna2_1$	1.70	1747	3.9
$NaSbOGeO_4$	13.008(5)	6.433(2)	10.736(3)	$Pna2_1$	0.73	2328	2.6
$TlSbOGeO_4$ at T/K							
293	13.369(2)	6.668(1)	10.758(1)	*Pnan*	3.9	764	3.7
280	13.331(2)	6.659(1)	10.740(3)	*Pnan*	3.9	1705	7.7
253	13.368(3)	6.669(2)	10.767(3)	$Pna2_1$	3.9	1331	4.5
123	13.358(2)	6.664(1)	10.762(1)	$Pna2_1$	3.9	1429	4.3
$AgSbOSiO_4$ at T/K							
293	12.832(9)	6.331(4)	10.727(6)	$Pna2_1$	0.66	1300	4.3
973 + slow cooling	12.786(6)	6.305(5)	10.717(7)	$Pna2_1$	0.72	1133	5.1
673 + quenching	12.781(4)	6.307(2)	10.754(3)	*Pnan*	0.55	1148	4.8

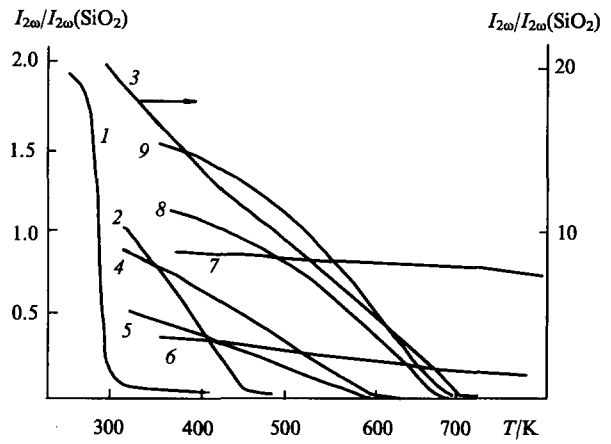


Figure 13. Temperature variation of the intensity of the second harmonic generation signal[7,44] for different powders: (*1*) $TlSbGeO_5$; (*2*) $RbSbGeO_5$; (*3*) $KTaGeO_5$; (*4*) $KSbGeO_5$; (*5*) $KSbSiO_5$; (*6*) $NaSbSiO_5$; (*7*) $NaSbGeO_5$; (*8*) $AgSbSiO_5$; (*9*) $AgSbGeO_5$.

$AMOXO_4$ (A = Na, K, Rb, Tl, Ag; M = Sb, Ta; X = Ge, Si) have been obtained recently and their structures have been investigated.[41,42] On the basis of results of measurements of the temperature dependence of the generation of the second harmonic of laser radiation[7] (Fig. 13), as well as dielectric and microcalorimetric studies,[43] the phase transitions were assigned to the class of second-order transitions. The possibility of a weak first-order transition has also been considered for $TlSbOGeO_4$ and $AgSbOSiO_4$.[44,45] The Curie points T_c, determined by various methods, agree satisfactorily and the entire group of compounds has as a whole significantly lower T_c than the phosphates and arsenates known up to that time.

The study of the phase transitions in new compounds of the $KTiOPO_4$ structural type makes it possible to discover the structural features responsible for the ferroelectric and nonlinear optical properties. According to the results of measurements of second harmonic generation (SHG), the crystal structures of K,Sb germanate, Rb,Sb germanate, K,Ta germanate, and also $NaSbOGeO_4$ obtained from $KSbOGeO_4$ by ion exchange in a $NaNO_3$ melt (the sold-phase synthesis affords a sphene structure) proved to be polar (Table 7) like that of $KTiOPO_4$.[41,45–47] According to the results of French investigators,[48,49] Na, Sb and K, Sb silicates are also polar at room temperature with the space group $Pna2_1$.

The study of the crystal structures of $KFeFPO_4$ and $KSnOPO_4$ showed that the mixed framework made up of Fe(Sn) octahedra and P tetrahedra possesses a pseudosymmetry corresponding to the space group *Pnan* (Fig. 14).[50,51] It follows from this that there is a possibility that a highly symmetrical prototype phase may exist. SHG measurements have shown[7] that Tl, Sb germanate should have the structure of the centrosymmetric modification at room temperature, since T_c = 272 K for this compound.

The structure of $TlSbOGeO_4$ at room temperature has been investigated by Belokoneva and Mill'[52] and then reinvestigated by Belokoneva et al.[53] Within the framework of the *Pnan* group, the position of the Tl atom was found to be split (the Tl – Tl′ distance is 0.6 Å for populations of 0.65 and 0.35 respectively). The splitting of the positions of the cations in the large cavities of the mixed framework made up of M octahedra and P tetrahedra was first established for $KFeFPO_4$ and $KTiOPO_4$, where additional split positions were noted for the K(1) and K(2) atoms but with significantly smaller populations: 0.1 (in the additional position) compared with 0.9 (in the main position).[50] Crystal-chemical analysis showed that the splitting originates from the main positions along the direction of two additional pseudosymmetrical positions (Fig. 14).[52]

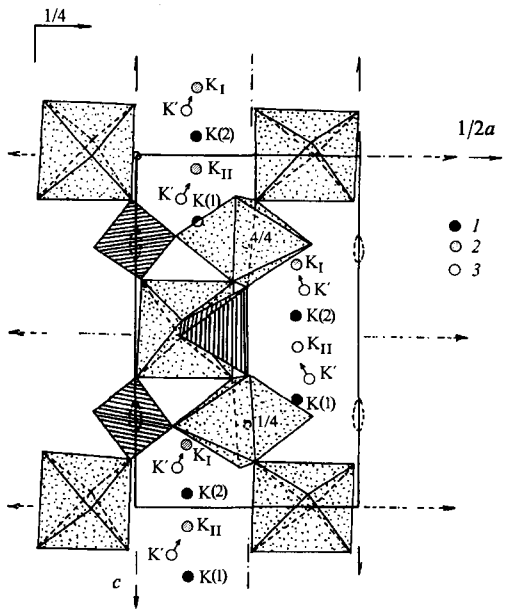


Figure 14. The pseudosymmetry of the framework in $KTiOPO_4$-like phases. The continuous lines represent the true symmetry elements of the space group $Pna2_1$, while the dashed lines represent the symmetry pseudoelements of the space group *Pnan*: (*1*) principal positions of K atoms; (*2*) additional positions; (*3*) unoccupied pseudosymmetrical positions.

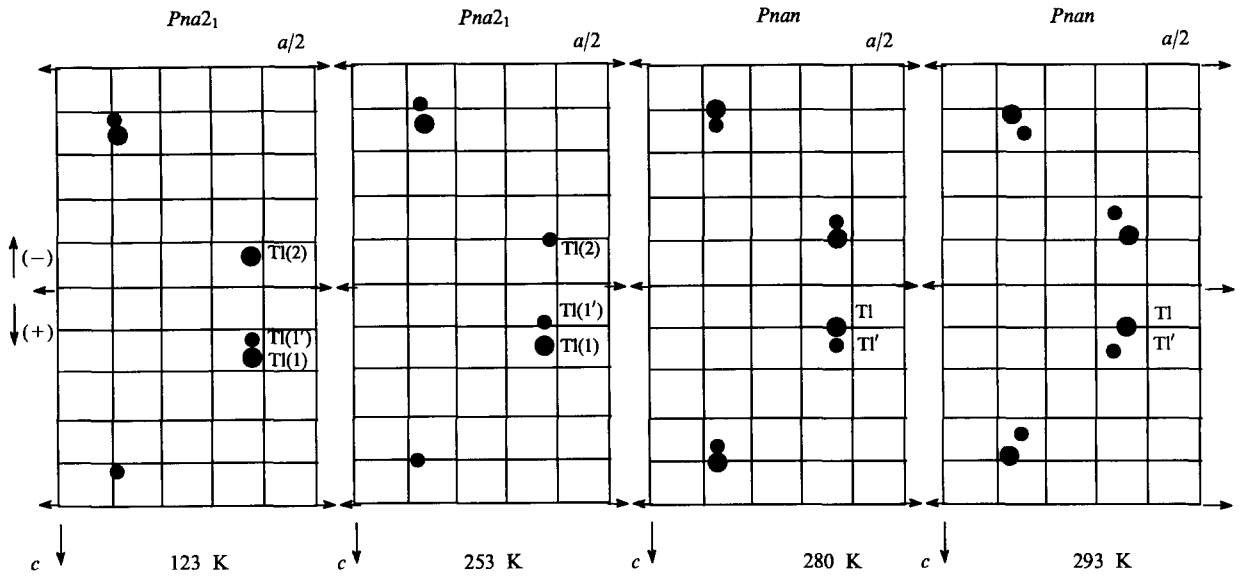


Figure 15. Disposition of Tl atoms at four temperatures in the $TlSbOGeO_4$ structure. The true axes in the space group *Pnan* and the twofold pseudoaxes in the space group $Pna2_1$ are shown at the 1/2 level on the *c* axis (at 123 and 253 K).

For the $TlSbOGeO_4$ crystal structure, the polar modification should exist also at a low temperature. It was expected that the Tl atoms would then be displaced from their positions in the structure to form an acentric modification. In order to determine the polar modification of the Tl, Sb germanate, low-temperature studies were carried out. At 123 K, the structure did indeed prove to be acentric[53] and the maximum displacement [to a greater extent for Tl(2) than for Tl(1)] was ~0.8 Å.

It was of interest to follow the dynamics of the phase transformation in the vicinity of the Curie point (272 K). For this purpose, a low-temperature X-ray diffraction experiment was carried out at 253 K. A study was also made of the structural state at 280 K, corresponding to an intermediate point between T_c and a second extremum at 286 K, observed in measurements of the relative permitivity and the electrical conductivity of $TlSbOGeO_4$ single crystals.[44] The results of the measurements and structural calculations at the above four temperatures are presented in Fig. 15 and Table 7.[53,54] The positions of the Tl atoms and the positions symmetrical to them in the two modifications are linked by either a true twofold axis or a twofold pseudoaxis. The distances from the ½ level along the *c* axis, (+) and (−), are given in Table 8. It is seen from the data in Table 8 that, compared with room temperature, the populations of the positions at 280 K remain unchanged, the atoms being slightly displaced towards the twofold axis. Overall, the structure determined from the system of sharp reflections (diffuse ring reflections with a texture similar to that of metals were also observed on the rocking X-ray diffraction pattern) retains the centrosymmetric space group and its principal characteristics. At 253 K, after passage through T_c = 272 K, the space group changes and becomes acentric, one of the Tl positions (−) is no longer split and the (+) and (−) distances are not strictly equal (Table 8), although they are in fact similar to one another [Tl(2) and Tl(1′)] and to the distances for the Tl and Tl′ positions at 280 K. The populations of the Tl–Tl′ positions (280 K) and Tl(1′)–Tl(1) positions (253 K) also change. With decrease in temperature, the polarity of the *c* axis increases owing to further displacement of the Tl atoms. The difference between the (+) and (−) distances increases and is now appreciably different from that in the initial (293 K) state (Table 8). As mentioned above, the overall shift is ~0.8 Å. The thermal corrections for the Tl and O atoms at 253 K indicate the instability of the structure near the phase transition.

One may conclude that the thallium atoms are most responsible for the paraelectric⇆ferroelectric phase transitions. The calculated displacements of the remaining atoms of the structure are an order or two orders of magnitude smaller.[54] The phase transitions are most probably mixed second-order phase transitions, being simultaneously of the displacement and order–disorder type, since not only are the thallium atoms displaced but there is a change in the splitting of the positions and their populations [Tl(1) ⇆ Tl(1′)]. The appearance of structural polarity along the *c* axis is directly responsible for the occurrence of the spontaneous polarisation P_s in the same direction, which has been attributed to the manifestation of ferroelectric and nonlinear optical properties. We may note that a high ionic conductivity is characteristic of $TlSbOGeO_4$.

Such treatment of the structural transformations is consistent with the approaches developed by Abrahams[2] in order to account for the structure–ferroelectric properties relation. The Abrahams–Kurtz–Jamieson (AKJ) criterion relates the square of the maximum displacement of the atom along the polar direction from the position with zero spontaneous polarisation to the

Table 8. The distances between the Tl atoms in $TlSbOGeO_4$ and the true twofold axis or twofold pseudoaxis.

Atom	Space group $Pna2_1$		Atom	Space group *Pnan*	
	123 K	253 K		280 K	293 K
			Tl′	−0.1441 (1.55)	−0.1502 (1.62)
Tl(2)	−0.0827 (0.89)	−0.0985 (1.06)	Tl	−0.0959 (1.03)	−0.1029 (1.11)
Tl(1′)	−0.1242 (1.34)	+0.0938 (1.01)	Tl	+0.0959 (1.03)	+0.1029 (1.11)
Tl(1)	+0.1562 (1.68)	+0.1464 (1.58)	Tl′	+0.1441 (1.55)	+0.1502 (1.62)

Note. Values expressed as fractions of the cell are quoted, the same values in Ångstroms being given in brackets.

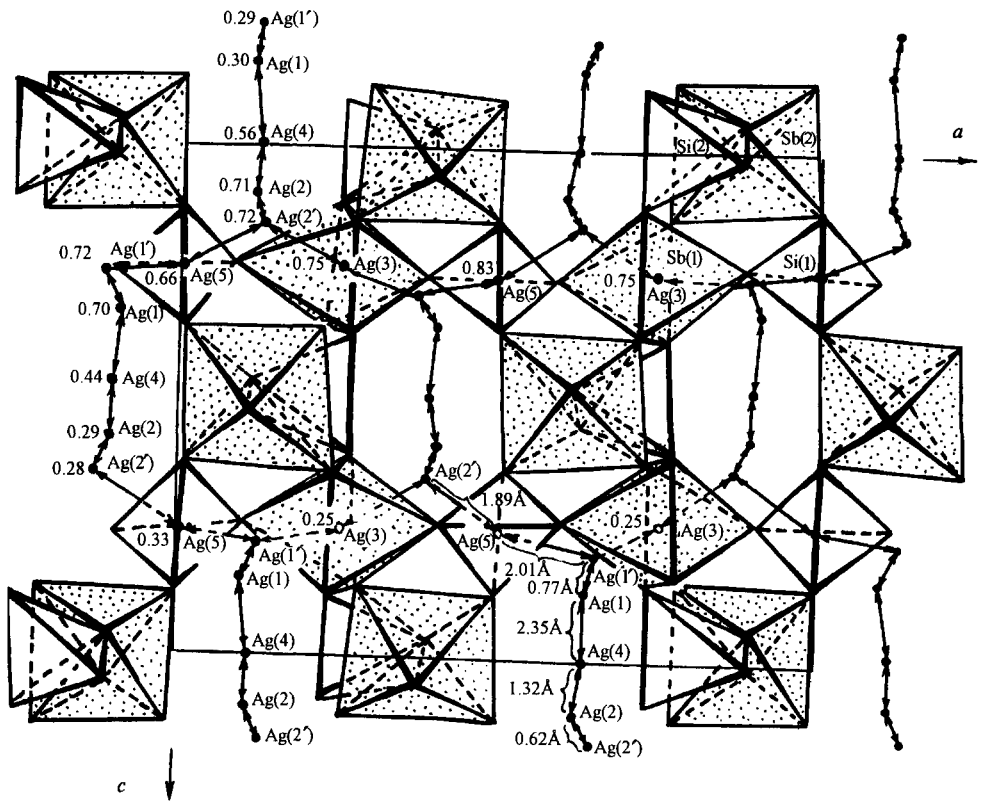


Figure 16. The cation migration pathways in $AgSbOSiO_4$ (projection onto the *ac* plane). The heights of the atoms and the distances between the positions in the independent increment are shown.

Curie point T_c.[2] According to this criterion, the group of germanates investigated, belonging to the $KTiOPO_4$ structural type and having in the polar state a higher pseudosymmetry than $KTiOPO_4$ and other phosphates and arsenates, should be distinguished by smaller atomic displacements in phase transitions and should have a correspondingly lower Curie point T_c, which has in fact been observed in measurements.

The higher pseudosymmetry and the very slight distortion of the octahedra in the germanates investigated (with which the non-linear optical properties are traditionally associated) compared with the Ti octahedra in $KTiOPO_4$ are responsible for the significantly lower intensity of the SHG signal in these compounds than in 'record holders' such as $KTiOPO_4$ and $KTiOAsO_4$.

The results of the study of the $AgSbOSiO_4$ structure (Table 7) constitutes an extremely remarkable example confirming that the cations in compounds of the given structural type are responsible for the course of the phase transitions and the ionic conductivity. Like $NaSbOGeO_4$ crystals, those of $AgSbOSiO_4$ have been obtained by ion exchange in a nitrate melt.[45] Despite the clear acentricity of the structure at room temperature, both positions, Ag(1) and Ag(2), are split, the components having similar populations, as in the case of $TlSbOGeO_4$, i.e. the Ag atoms occupy virtually all four possible positions[50,55] for cations in the cavities. The electron density difference maps unexpectedly show peaks at positions corresponding to cavities joining the large cavities within the skeleton, i.e. to passages between the tetrahedra and octahedra and also at the centres of the largest cavities between the four positions occupied by cations. This made it possible to discover the real ion-exchange channels. Previously their existence in structures of the $KTiOPO_4$ type was merely postulated in view of the manifestation of ion-exchange properties by the latter.[56]

Fig. 16 illustrates the ion-exchange channels in the $AgSbOSiO_4$ structure. The Ag(5) position, located in the widest passages between the tetrahedra, is populated to the greatest extent in the structure (population coefficient $f = 0.07$). Some of the silver atoms have 'settled' at the centres of the cavities at the Ag(4) position ($f = 0.04$). Traces of silver have been detected also at the Ag(3) position ($f = 0.01$) in the narrower passages between the more bulky octahedra (compared with tetrahedra). Accordingly, the populations of the three principal positions of the Ag atoms in the structure are found to be deficient.

The schematic representation of the potential relief profile in Fig. 17 for the principal conductivity channel along the *c* axis

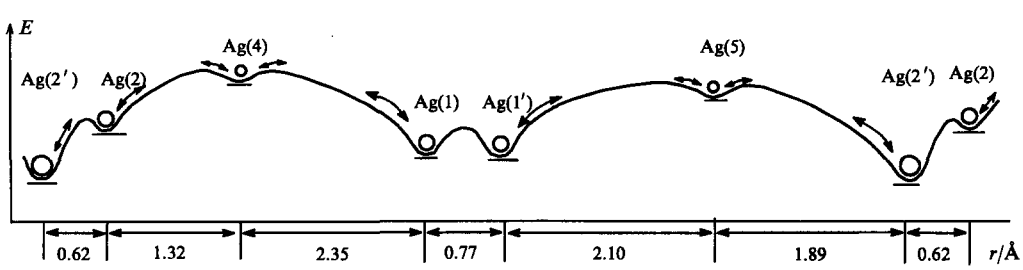


Figure 17. Schematic profile of the potential relief of the main ion-exchange channel in the $AgSbOSiO_4$ structure.

(a second possible path is along the *a* axis; there is no path along the *b* axis) illustrates the jumps of Ag atoms during ion migration. This state is unstable and one may expect that, for example on heat treatment of the crystals, the Ag(3, 4, 5) positions will be vacated.

Annealing of the specimens with subsequent quenching and slow cooling yielded interesting results. Slow cooling from 973 K leads to the same polar structure but with vacated Ag(3, 4, 5) positions and with some redistribution of the silver atoms relative to the initial ion exchange state at the main positions.

Fixation by quenching at 673 K afforded the high-temperature centrosymmetric modification. In contrast to the positions of the Tl atoms in $TlSbOGeO_4$, the positions of the Ag atoms in $AgSbOSiO_4$ (space group *Pnan*) are hardly split (f = 0.02) (Fig. 18). The population of the position corresponding to the tetrahedral passage diminished appreciably and the positions at the centre of the cavity and between the octahedra were vacated.

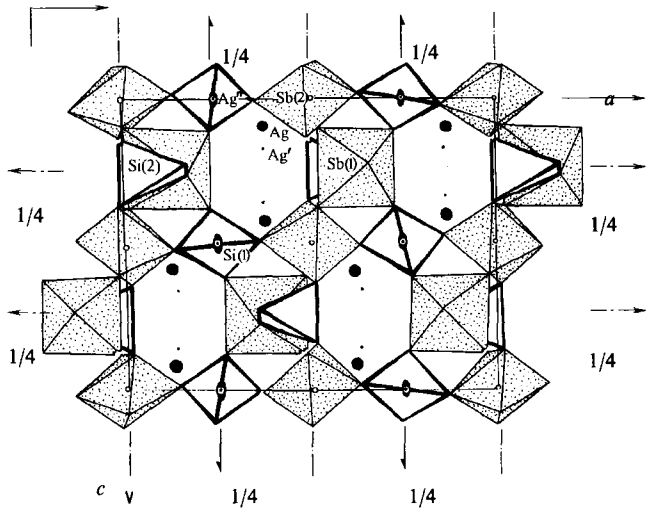


Figure 18. Projection of the centrosymmetric modification of $AgSbO.SiO_4$ onto the *ac* plane after annealing at 673 K and quenching. The positions of the Ag atoms and the symmetry elements of the space group *Pnan* are shown.

The course of the phase transformations in $AgSbOSiO_4$ is also reflected in Fig. 19, where the state at 293 K and that quenched at 673 K are the extreme possible states, while the state obtained on slow cooling from 973 K is intermediate. The Ag(2′)–Ag(2′)–Ag positions populated to the maximum extent are retained together with the Ag(1)–Ag(1)–Ag positions. The Ag(1) position (973 K) begins to split only on cooling, but does not return to the initial state Ag(1′) at 293 K. The pseudosymmetry of the crystal annealed at 973 K is much higher than the pseudosymmetry of the crystal cooled to 293 K. This is also seen from the comparison of the coordinates of the (+) and (−) positions of the Ag atoms, as for the Tl atoms in the case of $TlSbOGeO_4$.

This confirms the conclusion reached previously for the Tl compound that the disposition of the cations in the cavities of structures of the $KTiOPO_4$ type is the principal determinant of their symmetry and hence of their properties. X-Ray diffraction studies [55] made it possible for the first time to locate the pathways followed in the migration of the cations in structures of the $KTiOPO_4$ type and to explain the preferred conduction along the *c* axis, the weak conduction along the *a* axis, and its absence along the *b* axis.

A tetragonal pseudosymmetry is also characteristic of $KTiOPO_4$, which had been noted already by Tordjman et al. [57] The tetragonal modification has also been detected [58] for the compound $K(Mg_{1/3}Nb_{2/3})PO_5$. The results make it possible to conclude that the isomorphous substitutions play an important role in the manifestation of nonlinear optical properties, in particular that they are sharply impaired when Mg atoms are incorporated in the structure.

X. The sphene (titanite) structural type

As already mentioned above, the solid-phase synthesis of $NaSbOGeO_4$ leads to the sphene structure. This indicates a similarity of the regions corresponding to the existence of these two structural types. Among the four crystalline sphene structures (Table 9), only one has the $P2_1/c$ space group characteristic of the low-temperature modification. Note that $LiTaGeO_5$ has in addition a strongly pseudohexagonal symmetry [59] ($KTiOPO_4$-like phases have a pseudotetragonal symmetry). The formation of high-pressure modifications at

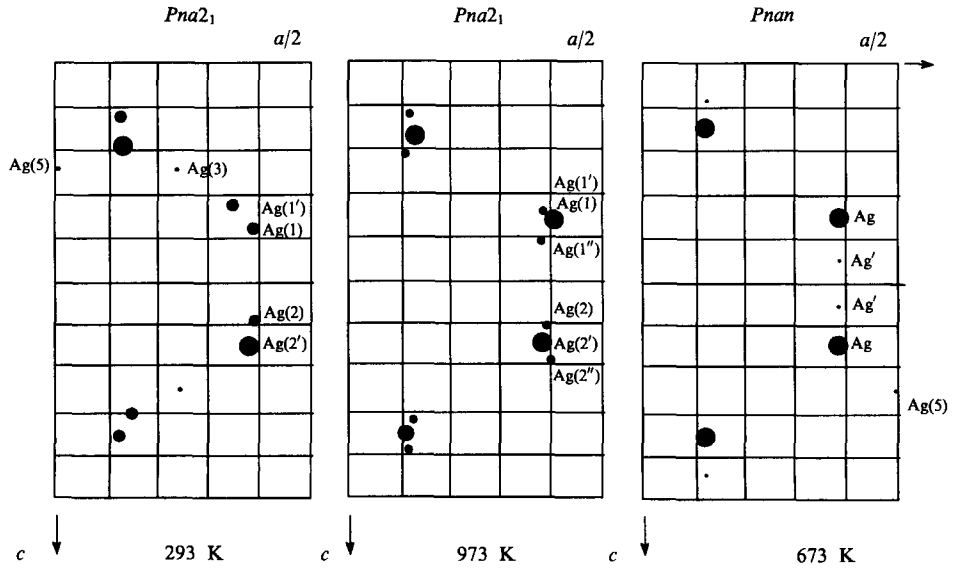


Figure 19. Disposition of the Ag atoms in the $AgSbOSiO_4$ structure at three temperatures.

Table 9. X-Ray diffraction characteristics of the phases investigated with structures of the sphene and sillimanite types.

Compound	a/Å	b/Å	c/Å	β	Space group	μr	N_{refl}	R_{hkl} (%)
$NaNbGeO_5$	6.798(4)	8.913(3)	7.523(2)	115.42	$P2_1/c$	0.7	2445	2.6
$NaTaGeO_5$	6.843(4)	8.916(4)	7.417(7)	114.77	$C2/c$	1.3	600	6.3
$LiTaGeO_5$	7.589(5)	8.130(4)	7.509(6)	119.55	$C2/c$	1.35	918	4.9
$NaSbGeO_5$	6.722(6)	8.892(7)	7.220(7)	114.76	$C2/c$	0.9	1517	3.3
$LiNbGeO_5$	7.738(1)	7.512(1)	6.706(6)	–	$Pnam$	1.1	1694	2.0

pressures significantly lower than for silicates is characteristic of germanates. The high-temperature modifications are formed with a $KTiOPO_4$ type of structure at much lower temperatures than, for example, those of phosphates. The sphene germanates also crystallise preferentially with the space group $C2/c$ (the high-temperature modification). The reason for this is the unusual crystal-chemical properties of the Ge atoms (large ionic radius, smaller electronegativity compared with Si), which are manifested, in particular, by the much greater ease of the formation of compounds with Ge atoms in the octahedra.

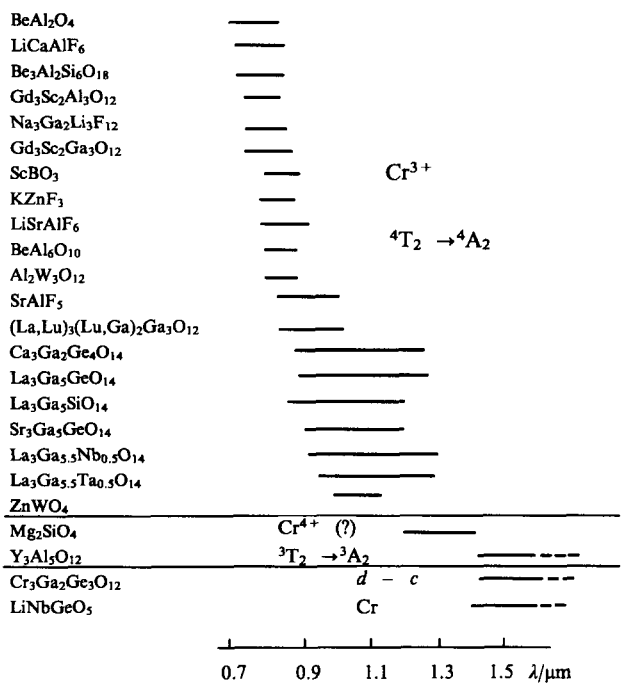


Figure 20. The spectral ranges corresponding to the retuning of the lasing wavelength for chromium-containing laser crystals.[61]

In the study of niobium-containing compounds, it was observed that the compound $LiNbGeO_5$ crystallises in the fairly unexpected sillimanite (Al_2SiO_5) type structure. The two structures are similar, when account is taken of the replacement of Li by Al, of Nb by Al, and of Ge by Si and of the change in the symmetry space group. Chains of Nb, Sb, and Ta octahedra, equivalent to the Ti octahedra in natural sphene, are differentiated in the $LiNbGeO_5$ structure, as in the sphene structure. According to the spectroscopic data of Dutch investigators[60] as well as our own data,[61] stimulated emission can be excited from $LiNbGeO_5$, especially in the presence of a Cr^{3+} admixture. Consequently, this crystal can be used in lasers. The spectroscopic characteristics of 24 chromium-containing compounds (Fig. 20) and of well known laser crystals (Y,Al and Gd, Sc garnets, fluorides, and oxides) and of the new phases examined in the present review have been compiled and compared.[61]

XI. Germanate-zeolites and zeolite-like germanates

In a study of compounds which are potential ferroelectric materials, Abrahams[2] considered also the crystal structure of natural cancrinite (space group $P6_3$). The germanium analogue of cancrinite was obtained by hydrothermal synthesis. Whilst retaining the size of the unit cell and the space group (Table 10), the synthetic Ge-cancrinite contains the octahedral $Ge(OH)_6^{2-}$ group instead of CO_3 (Fig. 21).[4] The positions occupied in the lattice by the Ge, Al, O(1, 2, 3, 4) as well as Na(1, 2) atoms are completely filled while the Ge^{VI} position is half-filled. The change in coordination from plane-trigonal for the C atom to octahedral for the Ge atom following the replacement of CO_3 by $Ge(OH)_6^{2-}$ induces a slight shift of the Ge atom from the position occupied by the C atom on the c axis. The positions of the water molecules in the structure have also been determined. It was found that the large cavity-channels along the c axis ensure the ion-exchange properties of the synthetic cancrinite. In natural cancrinite, these cavities are blocked by OH groups, while in the synthetic Ge-cancrinite the cavity is occupied by the $[Ge(OH)_6]^{2-}$ groups, which are, as it were, trapped by the structure—the $Ge(OH)_6$ octahedra had been observed earlier in the mineral stottite $Fe[Ge(OH)_6]$. Thus the synthetic germanium cancrinite possesses ion-exchange properties and is a potential ferroelectric material.

Table 10. X-Ray diffraction characteristics of the zeolite-germanates and zeolite-like germanates investigated.

Compound	a/Å	b/Å	c/Å	Space group	μr	N_{refl}	R_{hkl} (%)
Cancrinite	13.023(5)	–	5.204	$P6_3$	1.0	792	5.5
$Na_8Al_6Ge_6O_{24} \cdot Ge(OH)_6 \cdot 2H_2O$	–	–					
Sodalites							
$Na_8Al_6Ge_6O_{24}(OH)_2$	9.029(5)	–		$P\bar{4}3n$	1.0	455	4.8
$Na_8Al_6Ge_6O_{24} \cdot (Br_{1.5}OH_{0.5})$	9.089(1)	–		$P\bar{4}3n$	1.0	495	5.1
$K(H_3O)_3Ge_7O_{16}$	7.707(4)			$P\bar{4}3n$	0.6	220	6.8
$Rb_3Sb_3[Si_3O_9]O_6$	7.296(2)	10.295(2)	20.166(4)	$P2_12_12_1$	1.3	2070	4.1
$Cs_4Sb_4[Ce_4O_{12}]O_8$	7.240(2)		20.022(5)	$P\bar{4}m2$	1.8	1328	7.6
$K_{3.8}Nb_5[Ge_3O_9]O_{11.4}$	7.064(2)	12.177(2)	22.113(5)	$Pbc2_1$	1.0	1637	7.9

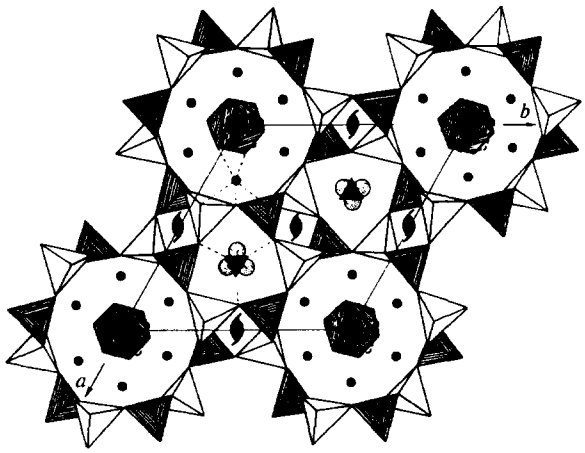


Figure 21. Projection of the structure of Ge-cancrinite onto the *ab* plane.

Sodalite also has germanium analogues (Table 10)[62,63] in which the positions of the Al, Na, and O (1, 2) atoms are retained while the Si atom is replaced by Ge. In the Ge-hydrosodalite, the OH groups of the natural mineral have been displaced from the 2*a*(000) positions of the Cl atoms to the 8*e*(*xxx*) positions and, for a statistical distribution, there is one OH group per cavity. The positions of the Br atoms are identical with those of the Cl atoms. Isomorphous substitutions in the anionic component makes it possible to improve the cathodochromic properties. Sodalites may prove promising for use where crystals with electrooptical and piezoelectric properties are required.[63]

Zeolites having the composition $M_3HGe_7O_{16} \cdot 4H_2O$ were described by Novotnyi[64] as early as 1958. It was noted that the combination of Ge octahedra and tetrahedra leaves room for large channels in the direction of coordinate axes, while the alkali metal cations are distributed statistically. This accounts for the zeolitic properties of these phases. The Ge-zeolite investigated (Table 10) contains the atoms of potassium as the metal, the deficiency of K atoms being compensated by the excess number of H atoms (or H_3O^+ groups).[65] The structural type of the Ge-zeolite belongs to the leucophosphite–pharmacosiderite group. Thus the crystal structure of $Cs_3Mo_4P_3O_{16}$ in this family[66] may be compared with the structure of $K_3Ge_7O_{16} \cdot 4H_2O$ (investigated by Sturua et al.[65]), where the positions of the Ge(2) atoms in the octahedron have been occupied by Mo atoms, while those of the Ge(1) atoms in the tetrahedron have been occupied by P atoms. The Cs atom is at the centre of the large channels. The diameters of the channels are ~5 Å in the $Cs_3Mo_4P_3O_{16}$ zeolite, exceed 6 Å in cancrinite, and are ~4 Å in sodalites.

We shall examine a further three structures of germanates and a silicate having the general formula $AMTO_5$ with the alkali metals A = K, Rb or Cs, M = Nb or Sb, and T = Ge or Si. Whilst differing in symmetry (Table 10), all three crystals have one feature in common, namely the large cavities in which the A atoms are accommodated. These cavities communicate with one another via channels which facilitate the ion-exchange in these compounds.

In the orthorhombic $RbNbSiO_5$[67] containing the chain radical $[Si_3O_9]_\infty$, the mixed framework $\{Nb_3[Si_3O_9]\}^{6-}$ was obtained by combining the three-dimensional bands of Nb octahedra with Si chains (Fig. 22). The crystal contains tubular cavities, where Rb atoms are accommodated.

In the tetragonal $CsSbGeO_5$,[63] the pattern of the cross-junction of the octahedra (Fig. 23) is close to that in $RbNbSiO_5$. The difference is that in $CsSbGeO_5$ one series of apex-linked octahedra, located below the main rod, has been omitted. Furthermore, the octahedra in this compound form a framework and no longer a band. In this framework, joined to the four-membered $[Ge_4O_9]$ rings, there are large communicating cavities in which Cs atoms are accommodated (Fig. 24), and it is possible to

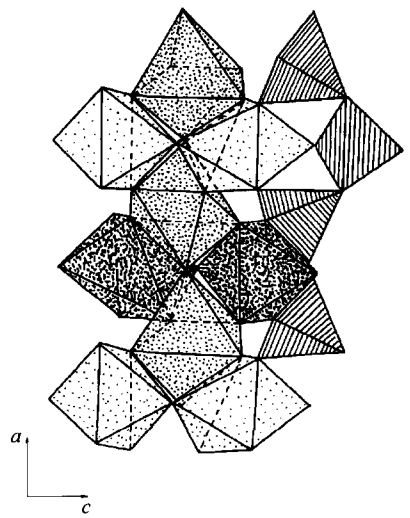


Figure 22. A band of Nb octahedra in the $RbNbSiO_5$ structure. The dot density reflects the height of the Nb octahedra along the *b* axis; the Si tetrahedra in the $[Si_3O_9]_\infty$ chain are shown shaded.

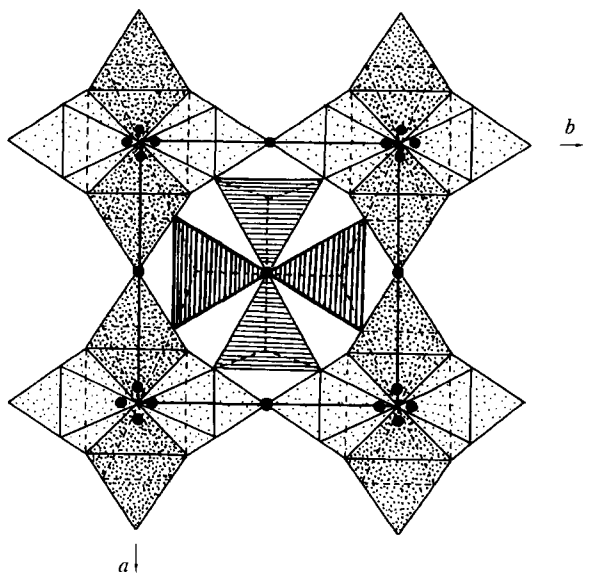


Figure 23. Projection of the $CsSbGeO_5$ structure onto the *ab* plane. The dot density reflects the height of the Sb octahedra along the *c* axis.

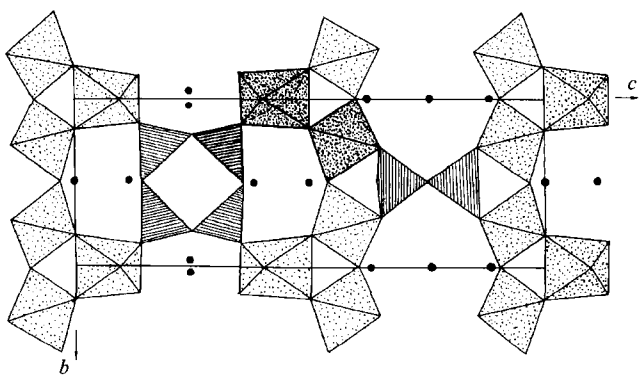


Figure 24. Projection of the $CsSbGeO_5$ structure onto the *bc* plane. The $KTiOPO_4$-like fragment is differentiated.

differentiate fragments close to the $KTiOPO_4$-like phases and sphenes. The crystal structure of $CsSbGeO_5$ was also solved in another study,[69] where the likely usefulness of this compound as an ion exchanger was likewise noted.

The crystal structure of the orthorhombic '$KNbGeO_5$'[70] with a slight deficiency of potassium and oxygen atoms (Table 10) proved to be derived from the structure of hexagonal $Cs_8Nb_{10}.Si_6O_{41}$.[71] In both structures, the tetrahedral radical is a three-membered $[T_3O_9]$ (T = Si, Ge) ring. In the structures, it is possible to differentiate the benitoite and pyrochlore fragments. The reason for the distortion of the '$KNbGeO_5$' structure and for the decrease in its symmetry from hexagonal to orthorhombic is the replacement of the Si atom by the large Ge atom in the tetrahedral position. To maintain the structure, the $[Ge_3O_9]$ ring in '$KNbGeO_5$' must be greatly distorted compared with $[Si_3O_9]$ in $Cs_8Nb_{10}Si_6O_{41}$ in order fit in the framework which has also been 'compressed' by replacement of Cs the by K. Like the two phases described above, K,Nb silicate should exhibit ion-exchange properties, i.e. it is possible to identify channels for the migration of cations along the *b* and *c* axes of the crystal.

* * *

More than 50 structures of germanates, gallates, borates, and silicates have been examined in the present review. The class of germanates (gallates), which predominates, provides analogues of the known structures of the silicate type such as garnet, melilite, sphene, cancrinite, and sodalite. Borogermanates are analogues of the borosilicates stillvellite and datolite. The tendency of germanium to be involved in octahedral coordination, particularly when it is present in excess in the initial systems, is responsible for the wide variety of germanates and their ability to form new structural types such as $A_3M_xT_{6-x}O_{14}$. An important factor is that the formation of high-temperature modifications at lower temperatures than, for example, in the case of phosphates, is typical for germanates. This makes it possible to investigate successfully the phase transitions in $KTiOPO_4$-like phases.

The study of the structures of the new phases is extremely important for the interpretation of their physical properties and for the understanding of their nature and hence in the search for phases having these properties and for the improvement of the already existing physical characteristics, for example by means of isomorphism.

The crystals of germanates, gallates, borates, and silicates investigated have a wide range of physical properties and can serve as multifunctional elements in engineering.

References

1. G D Stucky, M L F Phillips, T E Gier *Chem. Mater.* **1** 492 (1989)
2. S C Abrahams *Acta Crystallogr., Sect. B* **46** 311 (1990)
3. B V Mill', A V Butashin, G G Khodzhabagyan, E L Belokoneva, N V Belov *Dokl. Akad. Nauk SSSR* **264** 1385 (1982)
4. E L Belokoneva, T G Uvarova, L N Dem'yanets *Kristallografiya* **31** 874 (1986)
5. E L Belokoneva, T I Timchenko *Kristallografiya* **28** 1118 (1983)
6. A A Kaminskii, B V Mill', G G Khodzhbagyan, A F Konstantinova, A J Okorochkov, I M Silvestrova *Phys. Status Solidi A* **80** 387 (1983)
7. B V Mill', S Yu Stefanovich, A V Butashin *Kristallografiya* **36** 1481 (1991)
8. F Bertaut, F Forrat *C. R. Hebd. Seances Acad. Sci.* **243** 382 (1956)
9. J E Geusic, H M Marcos, L G Van Hitert *Appl. Phys. Lett.* **4** 182 (1964)
10. G A Novak, G V Gibbs *Am. Mineralogist* **56** 791 (1971)
11. B V Mill', E L Belokoneva, M A Simonov, N V Belov *Problemy Kristallologii* (Problems of Crystallology) (Moscow: Izd. Mosk. Gos. Univ., 1982) p. 161
12. A A Kaminskii, B V Mill', A V Butashin *Phys. Status Solidi A* **78** 723 (1983)
13. A A Kaminskii, E L Belokoneva, A V Butashin, K Kurbanov, A A Markosyan, B V Mill', O K Nikol'skaya, S E Sarkisov *Izv. Akad. Nauk SSSR, Neorg. Mater.* **22** 1061 (1986)
14. N N Lobanov, V G Tsirel'son, E L Belokoneva *Zh. Neorg. Khim.* **33** 3021 (1988)
15. In *Fizika i Spektroskopiya Kristallov* (The Physics and Spectroscopy of Crystals) (Moscow: Nauka, 1986) Ch. 9, p. 197
16. In *Kristallokhimicheskaya Sistematika Mineralov* (Systematic Crystal-chemical Classification of Minerals) (Moscow: Izd. Mosk. Gos. Univ., 1985) p. 140
17. S Haussuhl, F Wallrafen, K Recker, J Eckstain *Z. Kristallogr.* **153** 329 (1980)
18. A A Kaminskii, E L Belokoneva, B V Mill', Yu V Pisarevskii, S E Sarkisov, I M Silvestrova, A V Butashin, G G Khodzhabagyan *Phys. Status Solidi A* **86** 345 (1984)
19. E L Belokoneva, N V Belov *Dokl. Akad. Nauk SSSR* **260** 1363 (1981)
20. A A Kaminskii, E L Belokoneva, B V Mill', S E Sarkisov, K Kurbanov *Phys. Status Solidi A* **97** 279 (1986)
21. P Korzak, F Raaz *Österr. Akad. Wiss. Sitzungen Math. Naturwiss. Klasse* **13** 383 (1967)
22. A A Kaminskii, E L Belokoneva, S E Sarkisov, K Kurbanov, B V Mill' *Izv. Akad. Nauk SSSR, Neorg. Mater.* **22** 1869 (1986)
23. A A Kaminskii, E L Belokoneva, B V Mill', K Kurbanov, E S Dosmagambetov, S A Tamazyan, A V Butashin *Izv. Akad. Nauk SSSR, Neorg. Mater.* **22** 2013 (1986)
24. A A Kaminskii, B V Mill', A V Butashin, E L Belokoneva, K Kurbanov *Phys. Status Solidi A* **103** 575 (1987)
25. E L Belokoneva, B V Mill', A V Butashin, A A Kaminskii *Izv. Akad. Nauk SSSR, Neorg. Mater.* **27** 1700 (1991)
26. A A Voronkov, Yu A Pyatenko *Kristallografiya* **12** 258 (1967)
27. S Yu Stefanovich, B V Mill', A V Butashin *Kristallografiya* **37** 965 (1992)
28. Y Uesu, N Horiuchi, E Osakabe, S Omori, B A Strukov *J. Phys. Soc. Jpn.* **62** 2522 (1993)
29. A Onodera, B A Strukov, A A Belov, S A Taraskin *J. Phys. Soc. Jpn.* **62** 4311 (1993)
30. A Callegary, G Ginseppetti, F Mazzi, C Tadini *N. Jb. Mineral. Mh.* **2** 49 (1992)
31. A A Kaminskii, A V Butashin, A Masljanizin *Phys. Status Solidi A* **125** 671 (1991)
32. E L Belokoneva, M A Simonov, A V Pashkova, T I Timchenko, N V Belov *Dokl. Akad. Nauk SSSR* **255** 854 (1980)
33. E L Belokoneva, A V Pashkova, T I Timchenko, N V Belov *Dokl. Akad. Nauk SSSR* **261** 361 (1981)
34. E L Belokoneva, A V Azizov, N I Leonyuk, M A Simonov *Zh. Strukt. Khim.* **22** 196 (1981)
35. E L Belokoneva, L I Al'shinskaya, M A Simonov, N I Leonyuk, T I Timchenko, N V Belov *Zh. Strukt. Khim.* **19** 382 (1978)
36. E L Belokoneva, L I Al'shinskaya, N I Leonyuk, M A Simonov, N V Belov *Zh. Strukt. Khim.* **20** 542 (1979)
37. K Dornberger-Schiff *Grundzüge einer Theorie der OD-Strukturen aus Schichten* (Berlin: Deutsch. Akad. Wissensch., 1964)
38. B B Zvyagin, E L Belokoneva *Kristallografiya* **29** 291 (1989)
39. E A Pobedimskaya, D Yu Pushcharovskii, O G Karpov *Strukturnye Tipy Redkozemel'nykh Silikatov, Germanatov i Fosfatov* (Structural Types of Rare-earth Silicates, Germanites and Phosphates) (Moscow: Izd. Mosk. Gos. Univ., 1984)
40. E L Belokoneva, L I Leonyuk, A V Pashkova, T I Timchenko *Kristallografiya* **33** 1287 (1988)
41. E L Belokoneva, B V Mill', A V Butashin *Izv. Akad. Nauk SSSR, Neorg. Mater.* **27** 1708 (1991)
42. C Pagnoux, D Guyomard, A Verbaere, Y Piffard, M Tournoux *C. R. Acad. Sci., Ser. 2* **312** 611 (1991)
43. A Simon, J Ravez, J F Favard, A Verbaere, Y Piffard *C. R. Acad. Sci., Ser. 2* **317** 179 (1993)
44. S Yu Stefanovich, B V Mill', A V Butashin *Kristallografiya* **38** 121 (1993)
45. B V Mill', A V Butashin, S Yu Stefanovich *Zh. Neorg. Khim.* **38** 947 (1993)
46. J F Favard, A Verbaere, Y Piffard, M Tournoux *C. R. Acad. Sci., Ser. 2* **315** 305 (1992)
47. E L Belokoneva, B V Mill' *Zh. Neorg. Khim.* **37** 998 (1992)

48. M P Crosnier, D Guyomard, A Verbaere, Y Piffard *Eur. J. Solid State Inorg. Chem.* **27** 845 (1990)
49. C Pagnoux, J F Favard, A Verbaere, Y Piffard, M Tournoux *C. R. Acad. Sci., Ser. 2* **314** 151 (1992)
50. E L Belokoneva, O V Yakubovich, V G Tsirel'son, V S Urusov *Izv. Akad. Nauk SSSR, Neorg. Mater.* **26** 595 (1990)
51. P A Thomas, A M Glazer, B E Watts *Acta Crystallogr., Sect. B* **46** 333 (1990)
52. E L Belokoneva, B V Mill' *Zh. Neorg. Khim.* **37** 252 (1992)
53. E L Belokoneva, F M Dolgushin, M Yu Antipin, B V Mill', Yu T Struchkov *Zh. Neorg. Khim.* **38** 631 (1993)
54. E L Belokoneva, F M Dolgushin, M Yu Antipin, B V Mill', Yu T Struchkov *Zh. Neorg. Khim.* **39** 40 (1994)
55. E L Belokoneva, B V Mill' *Zh. Neorg. Khim.* **39** 355; 363 (1994)
56. S Furusava, H Hayasi, H Y Ishibashi, A Mijamoto, T Sasaki *J. Phys. Soc. Jpn.* **62** 181 (1993)
57. P A Tordjman, R Masse, J C Guital *Z. Kristallogr.* **139** 103 (1974)
58. E M McCarron III, J C Calabrese, T E Gier, L K Cheng, C M Foris, J D Bierlein *J. Solid State Chem.* **102** 354 (1993)
59. B V Mill', E L Belokoneva, A V Butashin *Kristallografiya* **35** 316 (1990)
60. G Blasse, G J Dirksen *J. Solid State Chem.* **65** 283 (1986)
61. A A Kaminskii, B V Mill', E L Belokoneva, A V Butashin *Izv. Akad. Nauk SSSR, Neorg. Mater.* **27** 1899 (1991)
62. E L Belokoneva, L N Dem'yanets, T G Uvarova, N V Belov *Kristallografiya* **27** 995 (1982)
63. E L Belokoneva, T G Uvarova, L N Dem'yanets *Kristallografiya* **30** 800 (1985)
64. Kh Novotnyi *Usp. Khim.* **27** 996 (1958)
65. G Sturua, E L Belokoneva, M A Simonov, N V Belov *Dokl. Akad. Nauk SSSR* **242** 1078 (1978)
66. R C Haushalter *J. Chem. Soc., Chem. Commun.* 1566 (1987)
67. E A Genkina, E L Belokoneva, B V Mill', A V Butashin, B A Maksimov *Kristallografiya* **37** 606 (1992)
68. E L Belokoneva, B V Mill', A V Butashin *Zh. Neorg. Khim.* **37** 2435 (1992)
69. C Pagnoux, A Verbaere, A Kanno, Y Piffard, M Tournoux *J. Solid State Chem.* **99** 173 (1992)
70. E L Belokoneva, A V Butashin, B V Mill' *Zh. Neorg. Khim.* **38** 1455 (1993)
71. M P Crosnier, C Pagnoux, D Guyomard *Eur. J. Solid State Inorg. Chem.* **28** 71 (1991)